

**THERMAL DESIGN METHOD OF BAYONET TUBE HEAT
EXCHANGERS**

**A THESIS SUBMITTED TO THE GRADUATE
SCHOOL OF APPLIED SCIENCES
OF
NEAR EAST UNIVERSITY**

**By
DAHIRU USMAN**

**In Partial Fulfillment of the Requirements for
The Degree of Master of Science
in
Mechanical Engineering**

NICOSIA, 2016

DAHIRU USMAN

**THERMAL DESIGN METHOD OF BAYONET TUBE HEAT
EXCHANGERS**

**NEU
2016**

**THERMAL DESIGN METHOD OF BAYONET TUBE HEAT
EXCHANGERS**

**A THESIS SUBMITTED TO THE GRADUATE
SCHOOL OF APPLIED SCIENCES
OF
NEAR EAST UNIVERSITY**

**By
DAHIRU USMAN**

**In Partial Fulfillment of the Requirements for
The Degree of Master of Science
in
Mechanical Engineering**

NICOSIA, 2016

Dahiru Usman: THERMAL DESIGN METHOD OF BAYONET TUBE HEAT EXCHANGERS

**Approval of Director of Graduate School of
Applied Sciences**

Prof. Dr. İlkay SALİHOĞLU

**We certify that this thesis is satisfactory for the award of the degree of
Master of Science in Mechanical Engineering**

Examining Committee in Charge:

Assist. Prof. Dr. Cemal Govsa

Committee Chairman,
Mechanical Engineering Department , NEU

Assist. Prof. Dr. Ali Evcil

Mechanical Engineering Department, NEU

Prof. Dr. Nuri Kayansayan

Supervisor,
Mechanical Engineering Department, NEU

I hereby declare that all information in this document has been obtained and presented in accordance with academic rules and ethical conduct. I also declare that I have fully cited and referenced all material and results that are not original to this work, as required by these rules and conduct,

Name, Last name:

Signature:

Date:

ACKNOWLEDGEMENTS

I take this opportunity to express my sincere appreciation to my supervisor Prof. Dr. Nuri Kayansayan for his guidance and encouragement throughout the course of this thesis and also the staffs of mechanical engineering department Near East University.

I am indeed most grateful to my parents, relatives, and friends whose constant prayers, love, support, and guidance have been my source of strength and inspiration throughout these years.

I am obliged to thank my sponsor, my mentor Engr. Dr. Rabiou Musa Kwankwaso. His selfless government made our dreams a reality.

To my Family

ABSTRACT

The thermal design using effectiveness number of transfer unit (ε –NTU) method of bayonet tube heat exchanger operating under uniform heat transfer condition with constant outer surface wall temperature was described. Steady state fluid temperatures and the related boundary conditions are obtained from the energy balance on control volume of a bayonet tube. The temperature differential equations are transformed into dimensionless form, presented as a function of Hurd number (Hu), number of transfer unit (NTU), ratio of convective coefficient of outer tube surface (ξ) and flow arrangement. The dimensionless governing equations are solved simultaneously using fourth order Runge-Kutta method. The tube temperature distribution is obtained graphically over ranges of Hu and ξ for both flow arrangements satisfying exchanger energy balance. The effectiveness of the exchanger is determined as a function of shell side fluid temperature.

The temperature distribution shows that due to annulus high thermal conductance at a low value of Hu less heat is exchanged between the inner tube and the annulus, the bayonet tube behaves like single tube heat exchanger. The heat transfer to shell side is enhanced at high values of ξ . Reversing flow arrangement, results with higher heat transfer rates.

Keywords: Bayonet tube; heat exchanger; annulus; effectiveness; differential equations; energy balance; boundary conditions

ÖZET

Sabit dış duvar yüzey sıcaklığıyla tek tip ısı geçişi koşulu altında çalışan süngü boru ısı eşanjörünün etkenlik- geçiş birim sayısı (NTU) yöntemi kullanan termal tasarımı anlatılmıştır. Durağan durum akışkan sıcaklık ve ilgili sınır koşulları süngü borunun kontrol hacminde enerji dengesinden elde edilmiştir. Sıcaklık diferansiyel denklemleri ve sınır koşulları boyutsuz ısı ve akış uzunluğu kullanarak boyutsuz şekle dönüştürülmüştür. Boyutsuz sıcaklık, Hurd sayısı (Hu) fonksiyonu, geçiş birim sayısı (NTU), dış boru yüzeyinin konvektif katsayısı oranı (ξ) ve akış düzenlemesi olarak sunulmuştur. Boyutsuz sıcaklık diferansiyel denklemler dördüncü dereceden Runge-Kutta-yöntemi kullanılarak eş zamanlı olarak çözülmüştür. Boru sıcaklık dağıtımını eşanjörün enerji dengesini karşılayan her iki akış düzenlemesi için de Hu ve ξ aralıkları üzerinden grafiksel olarak elde edilir. Eşanjörün etkenliği gövde tarafı sıvı sıcaklığının bir fonksiyonu olarak belirlenmektedir.

Sıcaklık dağılımı boru içi ve halka arasında düşük bir Hu değerinde daha az ısı değişimi olduğunu göstermekte, bu da halka içinde yüksek termal iletkenliği olduğu ve süngü borunun tek boru ısı eşanjörü gibi davrandığı anlamına gelmektedir. Gövde içine ısı aktarımı yüksek ξ değerlerinde gerçekleşmektedir. Akış düzenlemesini tersine çevirmek daha yüksek ısı aktarım oranlarına neden olmaktadır.

Anahtar Kelimeler: Süngü boru; ısı eşanjörü, halka; etkenlik; diferansiyel denklemler; enerji dengesi; sınır koşulları

TABLE OF CONTENTS

ACKNOWLEDGEMENTS	i
DEDICATION	ii
ABSTRACT	iii
ÖZET	iv
TABLE OF CONTENTS	v
LIST OF TABLES	vii
LIST OF FIGURES	ix
LIST OF ABBREVIATIONS AND SYMBOLS	xi
CHAPTER 1: BACKGROUND	
1.1 Concept of Bayonet Tube Heat Exchanger.....	1
1.2 Literature Review.....	2
1.3 Objectives of the Research.....	5
1.4 Scope and Outline of the Research.....	5
CHAPTER 2: INTRODUCTION	
2.1 Tube Banks.....	7
2.1.1 Tube banks heat transfer.....	12
2.2 Heat Exchangers.....	12
2.2.1 Recuperators and regenerators.....	13
2.2.2 Heat transfer process	15
2.2.3 Geometry of construction.....	15
2.2.4 Heat transfer mechanism.....	16
2.2.5 Flow arrangement	16
2.3 Overall Heat Transfer Coefficient.....	17
2.3.1 Variable overall heat transfer coefficient.....	20

2.4 Heat Exchangers Design Methods.....	22
2.4.1 Logarithmic mean temperature difference (LMTD).....	23
2.4.2 Multi pass and cross flow heat exchanger (F-LMTD).....	25
2.4.3 Effectiveness- NTU method	26
2.4.4 Heat exchanger effectiveness(ϵ).....	27
2.4.5 Heat capacity ratio	30
2.5 Heat Transfer Dimensionless Numbers.....	30
2.5.1 Nusselt number (Nu).....	30
2.5.2 Prandtl number (Pr).....	31
2.5.3 Stanton number (St).....	31
2.5.4 Number of transfer unit (NTU).....	32
 CHAPTER 3: GOVERNING EQUATIONS AND BOUNDARY CONDITIONS	
3.1 Governing Equations Formulation and Boundary Conditions.....	33
3.1.1 Governing equations.....	33
3.1.2 Boundary conditions.....	34
3.1.3 Non-dimensionalization.....	34
3.2 Effectiveness	38
 CHAPTER 4: NUMERICAL TECHNIQUES	
4.1 Approximate Solution of Ordinary Differential Equations.....	39
4.1.2 Taylor's expansion approach.....	40
4.1.3 Runge-Kutta methods.....	41
4.2 Numerical Integration.....	41
4.3 Numerical Model of Governing Equations.....	42
 CHAPTER 5: RESULTS AND DISCUSSIONS	
5.1 Results and Discussions.....	45

CHAPTER 6: CONCLUSION

6.1 Conclusion..... 51

REFERENCES..... 52

APPENDICES

Appendix 1: Temperatures distribution for flow arrangement A..... 55

Appendix 2: Temperatures distribution for flow Arrangement B..... 64

Appendix 3: MATLAB program code for flow arrangement A..... 72

Appendix 4: MATLAB program code for flow arrangement B..... 75

LIST OF TABLES

Table 2.1: Constants C_1 for equation 1.....	10
Table 2.2: Correction factor C_2 for equation 1.2. $N_L < 20$ and $Re > 1000$	10
Table 6.1: Value of tip temperatures for flow arrangement A and B.....	50

LIST OF FIGURES

Figure 1.1: Bayonet tube heat exchanger and flow arrangements.....	2
Figure 1.2: Evaporator temperature distribution for flow arrangement A and B.....	3
Figure 1.3: Condenser temperature distribution for flow arrangement A and B.....	4
Figure 1.4: Evaporator effectiveness for flow arrangement A and B.....	4
Figure 1.5: Condenser effectiveness for flow arrangement A and B.....	5
Figure 2.1: Flow pattern for in-line tube bundles.....	7
Figure 2.2: Flow pattern for staggered tube bundles.....	8
Figure 2.3: Tubes banks arrangement arrangement.....	8
Figure 2.4: Recuperators type heat exchangers.....	13
Figure 2.4a: Fixed dual-bed regenerator.....	14
Figure 2.4b: Rotary regenerator.....	14
Figure 2.5: Types of heat exchanger based on heat transfer process.....	15
Figure 2.6: Types of heat exchanger based on geometry of construction.....	16
Figure 2.7: Types of heat exchanger based on heat transfer mechanism.....	16
Figure 2.8: Types of heat exchanger based on flow directions.....	17
Figure 2.9: Heat transfer through a plane wall.....	18
Figure 2.10: Hollow cylinder with the convective surface condition.....	18
Figure 2.11: Typical cases of heat exchanger with variable overall coefficient.....	21
Figure 2.12: Energy balance for parallel flow heat exchangers.....	23
Figure 2.13: Energy balance for counter flow heats exchangers.....	23
Figure 2.14: Temperature profile for counter flow heat exchanger.....	23
Figure 2.15: Temperature profile for parallel flow heat exchanger.....	24
Figure 2.16: Correction factor F for a shell and tube heat exchanger	26
Figure 2.17: Correction factor F for cross flow with both fluid unmixed.....	26
Figure 2.18: Temperature distribution in counter flows heat exchanger o.....	28
Figure 2.19: Effectiveness-NTU chart of heat exchangers.....	29
Figure 2.20: Laminar thermal boundary layer in a tube.....	32
Figure 3.1: The energy balance of bayonet tube heat exchanger section.....	33
Figure 4.1: Numerical solution of first order ordinary differential equation.....	40
Figure 5.1: Temperature pattern for flow arrangement A $Hu=0.5$ and $\xi = 0.6$	46

Figure 5.2: Temperature pattern for flow arrangement A $Hu=0.1$ and $\xi = 0.6$	46
Figure 5.3: Temperature pattern for flow arrangement B $Hu=0.5$ and $\xi = 0.6$	47
Figure 5.4: Temperature pattern for flow arrangement B $Hu=0.1$ and $\xi = 0.6$	47
Figure 5.5: Temperature pattern for flow arrangement A $Hu=0.1$ and $\xi = 0.9$	48
Figure 5.6: Temperature pattern for flow arrangement B $Hu=0.1$ and $\xi = 0.9$	49

LIST OF ABBREVIATIONS AND SYMBOLS

A:	Heat transfer surface area (m^2)
C_p:	Specific heat at constant pressure ($JKg^{-1}K^{-1}$)
d:	Tube diameter (m)
Hu:	Hurd number, equation (3.14)
h:	Heat transfers coefficient ($Wm^{-2}K^{-1}$)
i:	Enthalpy (J/kg)
k:	Thermal conductivity ($Wm^{-1}K^{-1}$)
L:	Tube length (m)
\dot{m}:	Mass flow rate ($kg s^{-1}$)
NTU_x :	Local number of transfer unit $[= \frac{h_{o1}P_{o1}}{mC_p} x]$
NTU:	Annulus number of transfer unit $[= \frac{h_{o1}A_{o1}}{mC_p}]$
ntu:	Inner tube number of transfer unit $[= \frac{U_2A_2}{mC_p}]$
p:	Perimeter (m)
\dot{Q}:	Heat transfer rate (J/s)
T:	Temperature (K)
U:	Overall heat transfer coefficient (Wm^2K^{-1})
X:	Non-dimensional flow length $[= \frac{h_{o1}P_{o1}}{mC_p} x]$
x:	Flow length (m)
ϵ:	Exchanger effectiveness
θ:	Nondimensional temperature
ξ:	Ratio of convective coefficient of outer tube surfaces $[= \frac{h_1}{h_{o1}}]$
Δ:	Difference
i:	Internal
In:	Inlet
j:	Nodal point
o:	External
w:	Wall
∞:	Shell condition

- 1:** Annulus conditions
- 2:** Inner tube conditions
- ex:** Exit

CHAPTER 1

BACKGROUND

1.1 Concept of Bayonet Tube Heat Exchanger

Heat transfer between two different temperature fluids is of great importance for most industrial processes, and the device design for such purposes is called heat exchanger and it's widely used in many applications such as chemical plant, refineries, food industries, air conditioning, refrigeration etc.

The main design constraints of industrial heat exchangers are tube stress, accessibility, systems dimensions and ease of maintenance, high tube stresses may result wear and tear thereby increasing financial cost. In certain applications in process industries heat exchangers failure may lead to a complete system shut down, hence, there is a need for a heat exchanger which is free from the above constraints (Minhas, 1993).

Bayonet tube heat exchanger is tubular form consisting of two concentric tubes, the inner tube open at both ends positioned inside the outer tube open only at one end as shown in Figure 1.1. The fluid can either flow by entering the inner tube and exiting annulus termed as flow A or flow B, through annulus and exit inner tube, the fluid flow is driven by the pressure difference between the inlet and outlet of bayonet tube, and it's suitable when the fluid to be heated or cooled is accessible from one side only and it's free from bending and axial compressive stresses (Minhas, 1993). Hurd in 1946 reported that the ease of replacement of individual tube of the bayonet tubes heat exchanger and expansion ability of bayonet tube are some unique advantages of bayonet tube heat exchanger, (Hurd, 1946).

Basically, the bayonet tube diameters represent for specified length of tubes the heat exchanger. The surface area, the cross-sectional area of inner and outer tubes are used in the determination of tubes side velocity and pressure drop for given flow rate of heat transfer fluid. The design of bayonet tube heat exchanger should focus in selecting suitable tubes diameter ratio to minimize the inner tube pressure drop and at the same time optimizing the heat transfer performance of the annulus (O'Doherty et al., 2001).

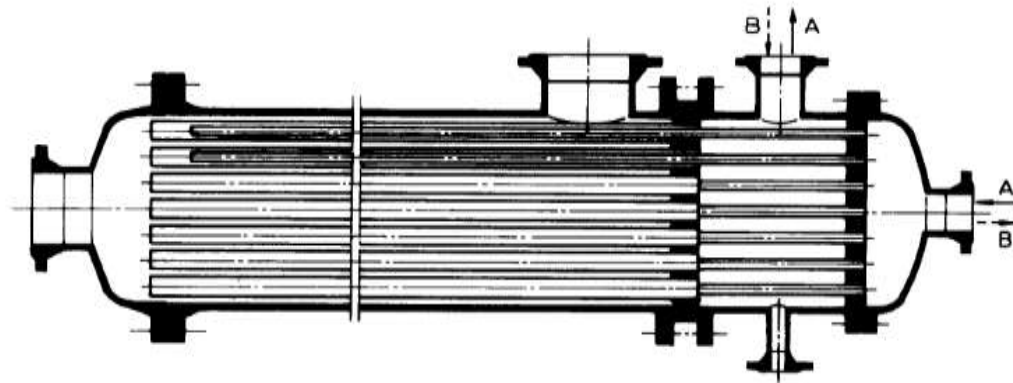


Figure 1.1: Bayonet tube heat exchanger and flow arrangements (Kayansayan, 1996)

1.2 Literature Review

The mean temperature difference distribution bayonet tube was first studied by Hurd in 1946, with unheated tube walls for four different shells and tube side flow arrangement. He found that large temperature differences were achieved for counter flow between the annulus and shell side fluids (Hurd, 1946). The test conducted by Jahns et al, in 1973, show that bayonet tube has the high rate of heat removal. Additionally, Haynes and Zerling in 1982 determined that the rate of heat removal of bayonet tube depends on the volume of air forced through the annulus.

The analytical results by Baum 1978, shows that the diameter of inner tube should be three quarters of outer tube diameter and a little thicker than outer tube. Lock and Kirchen 1988, recommended that the rate of heat transfer increase with the increase of outer tube length for high-velocity fluid, while opposite the case for low speed. In 1990 it is determined that that the effect of the length-diameter ratio of the outer tube on the rate of heat transfer was monotonic (Minhas, 1993).

Furthermore, Kayansayan (1996) from his thermal analysis of bayonet tube evaporators and condensers for pure fluids with variable wall superheat, the nonlinear governing equations was obtained by taking energy balance on bayonet tube control volume for constant shell temperature. The tube fluid temperature was determined to be function on four design parameters number of transfer unit (NTU), Hurd number (Hu), thermal resistance ratio ξ which is defined as $\xi = R_1/a/h_m$ and the flow arrangement. The effectiveness (ϵ) of the exchanger is a function of Hurd number, number of transfer unit and the flow arrangement.

The temperatures distribution for bayonet tube evaporators and condensers are obtained numerically over ranges of, $0 \leq Hu \leq 5$ and $10^{-5} \leq \xi \leq 10^{-1}$.

As shown in Figures 1.2 and 1.3, which indicate that for high values of Hurd number $Hu \geq 5$, the temperatures distribution shows minimum value which moves toward the tube tip as Hu increases. At the same design conditions, the evaporator performance was favored by flow arrangement B, in which the fluid enters through annulus and exit inner tube, the opposite case is true for the condenser, the exchanger effectiveness decrease with increase in Hu as shown in Figure 1.3. (Kayansayan, 1996). Accordingly, the present work would follow the same procedure for design analysis of bayonet tube heat exchangers with constant outer tube wall temperature.

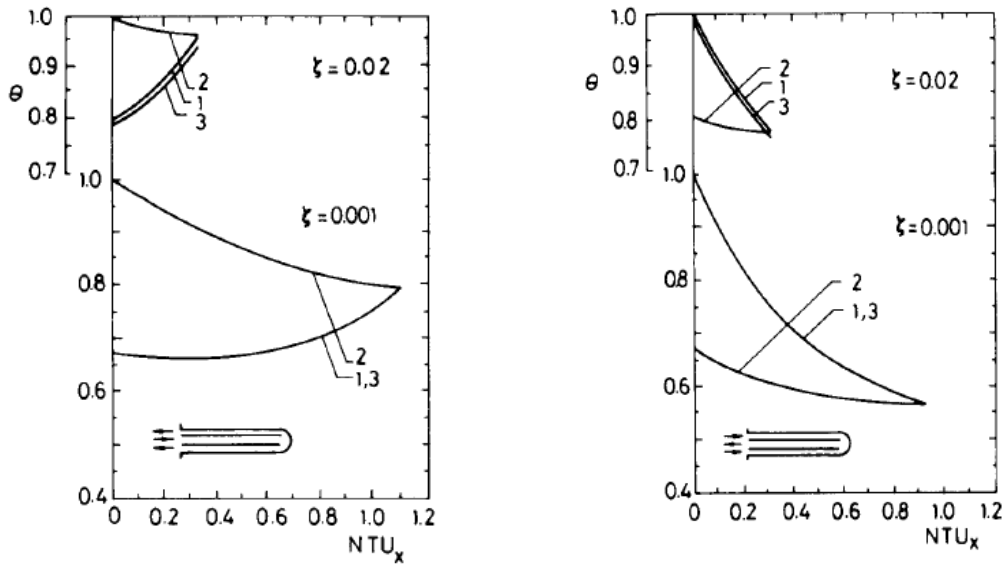


Figure 1.2: Evaporator temperature distribution for flow arrangement A and B. $Hu=1$,
 (1) θ_1 , (2) θ_2 , (3) θ_e (Kayansayan, 1996)

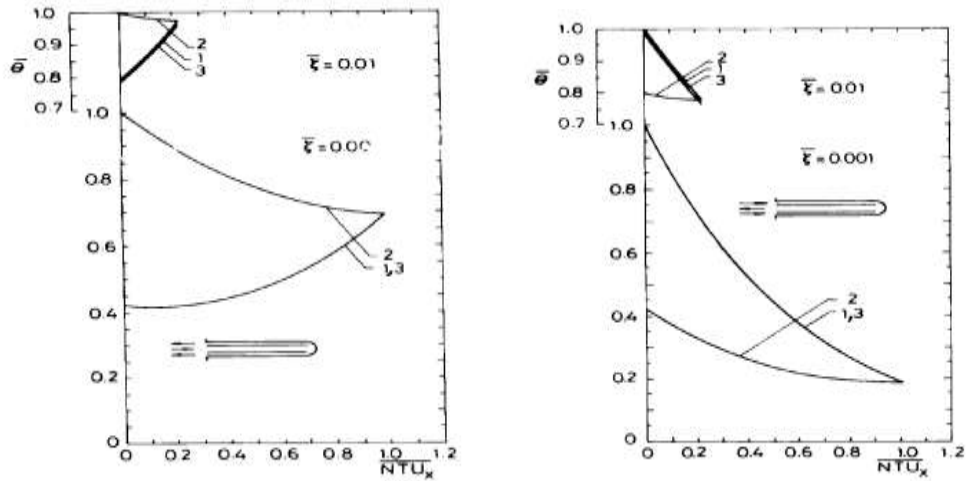


Figure 1.3: Condenser temperature distribution for flow arrangement A and B. $Hu=1$,
 (1) θ_1 , (2) θ_2 , (3) θ_e (Kayansayan, 1996)

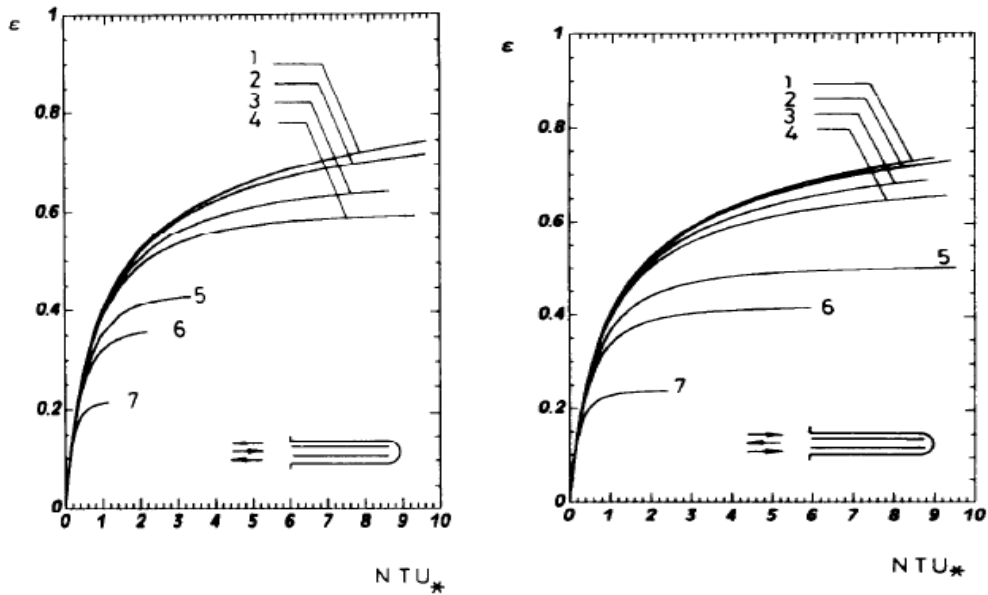


Figure 1.4: Evaporator effectiveness for flow arrangement A and B Hu (1) 0.01 (2) 0.01
 (3) 0.05 (4) 0.1 (5) 0.5 (6) 1 (7) 5 (Kayansayan, 1996)

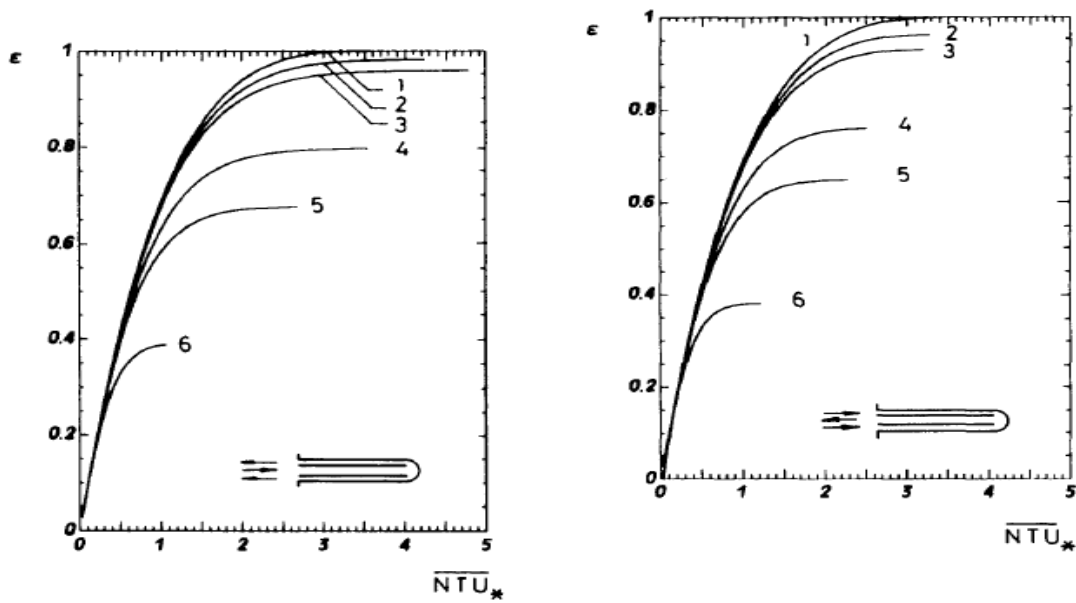


Figure 1.5: The Condenser effectiveness for flow A and B Hu (1) 0.01 (2) 0.01 (3) 0.05 (4) 0.1 (5) 0.5 (6) 1 (7) 5 (Kayansayan, 1996)

1.3. Objectives of the Research

The main objectives are,

- To determine the temperatures distribution of bayonet tube at given thermal conditions.
- To analyze the effect of the thermal design parameters.
- To determine the effectiveness of the exchanger.

1.4. Scope and Outline of the Research

Despite its unique advantages over conventional heat exchangers, the thermal design method developed earlier was based on the fact that the bayonet tube is operating under non-uniform heat transfer conditions along the outer tube surface with variable wall temperature. The present work considers uniform temperature along the outer tube surface. The outer tube surface wall temperature is assumed to be constant for this analysis. The governing equations are obtained from energy balance on control volume for steady and fully developed flow with a uniform heat transfer coefficient along the flow path. For a better understanding of the subject, Theory and some concepts of the heat exchanger and its design methods are explained in chapter 2.

In chapter 3, the energy equations and related boundary conditions are derived by taking energy balance on control volume of the bayonet tube under steady state conditions, the governing equations are transformed to dimensionless form through dimensionless temperatures and flow length.

Chapter 4 consist of a brief introduction to numerical solution methods and numerical modeling of governing equations. The governing equations are solved simultaneously using fourth order Runge-Kutta method together with the inlet and exit temperatures specified. The tubes temperatures distributions are obtained for ranges $0.1 \leq Hu \leq 0.5$ and $0.6 \leq \xi \leq 0.9$ satisfying energy balance for two possible flow arrangements, also the effectiveness of the exchanger is determined.

Chapter 5, presents the discussions of the results of temperatures distributions and the effect of design parameters are outlined.

Finally, conclusions and recommendations are contained in chapter 6.

CHAPTER 2

INTRODUCTION

2.1 Tube Banks

Analysis of fluid flow across tubes bank is essential in evaluating heat transfer for the design of commercial heat exchangers. In typical tubes bundle shown in Figure 2.1, the shell side fluid flows in between outer surfaces of tubes and the shell, there is speed up and the slowdown of the shell side fluid due to spontaneous changes in cross-sectional area along the flow path. The tube banks arrangement in the direction of flow velocity is of two type, the in-line and the staggered arrangements, as shown in Figure 2.2.

The configuration of tubes bank is characterized by the tube diameter D , the transverse pitch S_T and longitudinal pitch S_L measures between two tubes centers, as shown in Figure 2.2, (Theodore et al., 2002). According to Frank, the tube bundles heat transfer depends on boundary layer separation and wake interaction and increase considerably across the first fifth rows and slightly for the rest of the rows due negligible changes in flow conditions. (Frank et al., 2011). Due to decrease in the influence of upstream rows and downstream rows heat transfer is not enhanced at large S_L , Hence design of aligned tube bundles with $S_T/S_L < 0.7$ is undesirable, (Theodore et al., 2002).

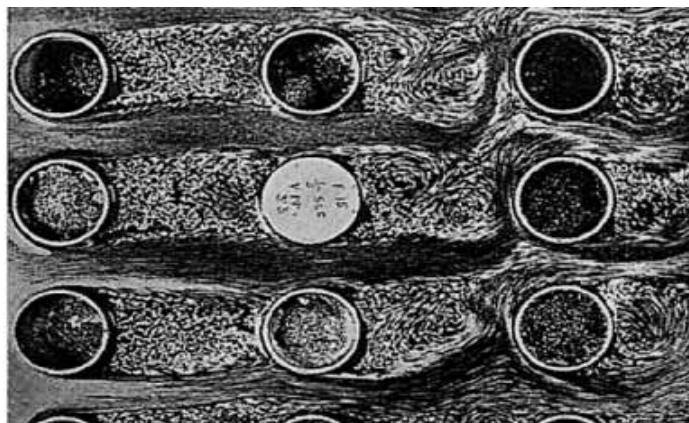


Figure 2.1: Flow pattern for in-line tube bundles (Frank et al., 2011).

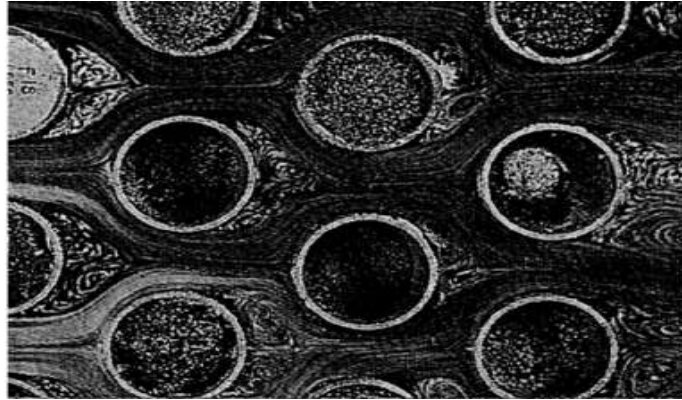


Figure 2.2: Flow pattern for staggered tube bundles (Frank et al., 2011)

In general, tube banks heat transfer is favored by the twisted flow arrangement of staggered tube bundles more especially at low Reynolds number ($Re \leq 100$). The relationship between heat transfer and energy dissipation depends largely on the fluid velocity, the size of the tubes and the distances between the tubes. The performance of closely spaced arrangement of staggered tubes is higher than in-line tube arrangement. (Frank et al., 2011). According to (Zukauskas and Ulinskas), Tube banks are classified as compact or widely spaced, a tube banks with pitch ratio ($a \times b \leq 1.25 \times 1.25$) is considered as compact and ($a \times b \geq 2 \times 2$) as widely spaced tube banks (Khan et al., 2006).

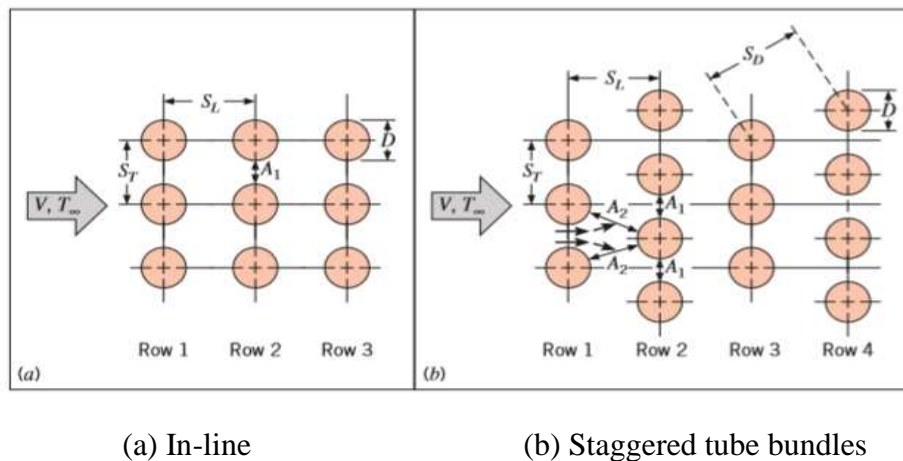


Figure 2.3: Tube banks arrangement in the flow direction

For thermal design analysis of tube bundles, the determination of average heat convective transfer coefficient expressed in term of a dimensionless number called Nusselt number (Nu) is of primary interest.

Zukauskas In 1972, proposed a correlation for the heat transfer across tube bundles with twenty or more rows in the flow direction as,

$$N_{\bar{u}} = C_1 R_{eD,max}^m P_r^{0.36} \left(\frac{P_r}{P_{rs}} \right)^{\frac{1}{4}} \quad (2.1)$$

For,

$$N_L \geq 20$$

$$0.7 \leq P_r \leq 500,$$

$$10 \leq R_{eD,max} \leq 2 \times 10^6$$

Where,

N_L is the number of rows measure in the flow direction

P_{rs} Prandtl number evaluated at tube wall temperature T_s , due to heat transfer to or from the tubes all others properties are evaluated at mean of inlet (T_i) and outlet an temperature of fluids (Theodore et al, 2002).

Similarly, for less than twenty rows, ($N_L < 20$) Equation (2.1) is corrected to

$$|N_{\bar{u}D}|_{(N_L < 20)} = |C_1 N_{\bar{u}D}|_{(N_L \geq 20)} \quad (2.2)$$

The constants C_1 , m and correction factor C_2 in Equation 2.1 and 2.2 can be determined from Tables 2.1 and 2.2 (Theodore et al, 2002).

The Reynolds number $Re_{D,max}$ in the Equations 2.1 and 2.2 is based on the maximum velocity occurring at the minimum free area between the tubes in the bundles.

$$R_{eDmax} = \frac{\rho V_{max} D}{\mu} \quad (2.3)$$

From Figure 2.2 for in-line arrangement, the maximum velocity occurs at transverse plane A_1 as

$$V_{max} = \frac{S_T}{S_T - D} \times V \quad (2.4)$$

Similarly, for staggered tubes arrangement, if S_L/S_T is small,

$$S_D = \sqrt{\left(S_L^2 + \left(\frac{S_T}{2} \right)^2 \right)} < \frac{S_T + D}{2} \quad (2.5. A)$$

Then the maximum velocity is given by

$$V_{max} = \frac{S_T}{S_D - D} \times V \quad (2.5. B)$$

V in the Equations 2.4 and 2.5, represent the free velocity of fluids. S_T is the distance between centers of two adjacent tubes in horizontal rows and measures perpendicular to the flow directions as shown in Figure 2.2, and S_L represents the distance between centers of adjacent transverse rows, in the flow directions as shown in Figure 2.2.

Table 2.1: Constants C_1 for Equation 2.1 (Theodore et al., 2002).

Configuration	$Re_{D,max}$	C_1	m
Aligned	$10-10^2$	0.80	0.40
Staggered	$10-10^2$	0.90	0.40
Aligned	10^2-10^3	Approximate as a single (isolated) cylinder	
Staggered	10^2-10^3		
Aligned ($S_T/S_L > 0.7$) ^a	$10^3-2 \times 10^5$	0.27	0.63
Staggered ($S_T/S_L < 2$)	$10^3-2 \times 10^5$	$0.35(S_T/S_L)^{1/5}$	0.60
Staggered ($S_T/S_L > 2$)	$10^3-2 \times 10^5$	0.40	0.60
Aligned	$2 \times 10^5-2 \times 10^6$	0.021	0.84
Staggered	$2 \times 10^5-2 \times 10^6$	0.022	0.84

^aFor $S_T/S_L < 0.7$, heat transfer is inefficient and aligned tubes should not be used.

Table 2.2: Correction factor C_2 for Equation 2.2. $N_L < 20$ and $Re > 1000$

N_L	1	2	3	4	5	7	10	13	16
Aligned	0.70	0.80	0.86	0.90	0.92	0.95	0.97	0.98	0.99
Staggered	0.64	0.76	0.84	0.89	0.92	0.95	0.97	0.98	0.99

In 2006, an analytical model was developed by Khan et al. The model can be used for wide ranges of parameters, as earlier correlations are restricted by specified values and ranges of longitudinal pitch, transverse pitch, Reynold's and Prandtl numbers of tube banks. In the analysis, average heat transfer coefficient of single tube selected from the first row of a tube banks was determined using Von Karman integral. The boundary layer analysis for isothermal conditions gives the heat transfer coefficient from separation point to rear stagnation point of a tube as (Khan et al., 2006),

$$N_{UDf1} = C_2 R_{eD}^{\frac{1}{2}} P_r^{\frac{1}{3}} \quad (2.6)$$

Also, from the experiments of (Zukauskas and Ziugzda) and Hegge Zijnen, it was determined that the heat transfer from the rear portion of the cylinder to the fluid can be obtained from,

$$N_{udf1} = 0.001R_{eD} \quad (2.7)$$

Therefore, the heat transfer coefficient of single tube selected from the first row of tube bundles can be determined by Equations 2.6 and 2.7, as (Khan et al., 2006),

$$N_{UDf} = C_2 R_{eD}^{\frac{1}{2}} P_r^{\frac{1}{3}} + 0.001R_{eD} \quad (2.8)$$

The constant C_2 depends on longitudinal a , transverse pitch b , and thermal boundary conditions, and is given by,

$$C_2 = \begin{cases} \frac{-0.016 + 0.6a^2}{0.4 + a^2} & \text{in - line} \\ \frac{0.588 + 0.004b}{((0.858 + 0.04b - 0.008b)\bar{a})^{\frac{1}{2}}} & \text{staggered} \end{cases} \quad (2.9)$$

For $1.25 \leq a \leq 3$ and $1.25 \leq b \leq 3$

Where,

$$\text{The longitudinal pitch } a = \frac{S_L}{D} .$$

$$\text{The transverse pitch } b = \frac{S_T}{D}$$

An experimental investigation by (Zukauskas and Ulinskas) shows that the average heat transfer of a tube in tube banks depends on tube location in the banks. The heat transfer of inner tube rows increase due to the turbulence generated by first row tubes, and the average heat transfer of the tube banks is given by,

$$N_{UD} = C_1 N_{UDf} \quad (2.10)$$

Where, the N_{UDf} is the heat transfer Nusselt number of first row tube, and C_1 coefficient derived from experimental data, and account for the dependence of average heat transfer on tube banks number of rows, for $R_{eD} > 10^3$, expressed as,

$$C_1 = \begin{cases} \frac{1.23 + 1.47N_L^{1.25}}{1.72 + N_L^{1.25}} & \text{in - line} \\ \frac{1.21 + 1.64N_L^{1.44}}{1.87 + N_L^{1.44}} & \text{staggered} \end{cases} \quad (2.11)$$

For number of rows $N_L \geq 16$, the values of $C_1=1.43$ for in-line and $C_1=1.61$ for staggered arrangements.

2.1.1 Tube banks heat transfer

The total rate of heat transfer \dot{Q} of the tube banks depends primarily on average heat transfer coefficient, inlet and outlet temperatures of the fluid and the heat transfer surface area as,

$$\dot{Q} = h(N\pi DL)\Delta T_{LM} \quad (2.12)$$

Where,

N is a total number of tubes in the bank,

N_T represent the number of tube in each row and ΔT_{LM} is log mean temperatures difference between bulk temperature of the fluid and tube wall temperature given by, (Khan et al., 2006).

$$\Delta T_{LM} = \frac{(T_s - T_i) - (T_s - T_o)}{\ln\left(\frac{T_s - T_i}{T_s - T_o}\right)} \quad (2.13)$$

T_i and T_o in Equation 1.7 represent inlet and outlet temperatures of the fluids, the outlet temperature is determined from energy balance of the tube banks as (Theodore, et. al, 2002),

$$\frac{T_s - T_o}{T_s - T_i} = \exp\left(-\frac{\pi DN\bar{h}}{\rho V N_T S_T C_P}\right) \quad (2.14)$$

The only unknown in Equation 2.13 and 2.14 is average convective heat transfer coefficient \bar{h} and can be determined using Equation 2.1 or 2.10.

The air outlet temperature and heat transfer rate can be increased by increasing the number of tube rows, or for fixed number of rows by adjusting the air velocity. The air outlet temperature would asymptotically approach surface temperature as a number of rows increases.

2.2 Heat Exchangers

Heat exchangers are devices that transfer heat from the high-temperature fluid to a fluid with low temperature, in order to control the temperature of one of the fluids for some certain purpose. The heat transfer between the fluids can be achieved by mixing the fluids involves directly or through a partition between the hot and cold fluid. The process of heat transfer is of two forms, convection heat transfer on the fluid side and conduction heat transfer by the separating wall, no work interactions or external heat in the heat exchanger. Heat exchangers are widely used in many applications such as power generation, food industries, chemical industries, refrigeration, air conditioning and waste water recovery, and it is classified based on the following criteria (Vedat, et al, 2000)

1. Recuperators/ regenerators
2. Transfer process (Direct contact and indirect contact)
3. Geometry of construction (tubes, plate and extended surfaces)
4. Heat transfer mechanism
5. Flow arrangement.

2.2.1 Recuperators and regenerators

In Recuperators heat exchanger the hot fluid recuperates (recovers) some heat from other fluid, the two fluids stream involves are separated by a wall or an interface through which heat is transferred between the fluids. The heat transfer involves convection between fluids and separating wall and the conduction through as separating wall which may include heat transfer enhancement devices such as fins. The recuperative heat exchanger is mainly classified as plate and tubular type.

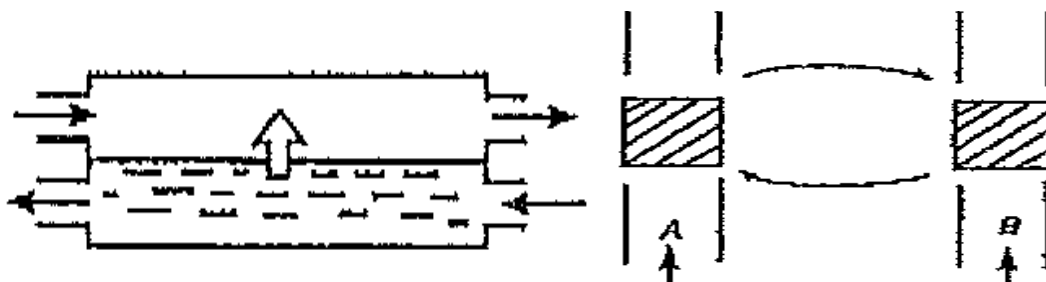


Figure 2.4. Recuperators type heat exchangers (Kakas and Liu, 2002).

A regenerators heat exchangers consist of a passage (matrix) which is occupied by one of the two fluids involves. Thermal energy is stored in the matrix by the hot fluid, during the cold fluid flow through the matrix extracts the energy stored by the hot fluid. The heat transfer is not through a wall as indirect type heat exchangers. Regenerators are used in a gas turbine, melting furnace, air pre-heater etc. (Kakas and Liu, 2002). For a fixed matrix configuration the hot and cold fluid passes through a stationary exchanger alternatively and two or more matrices are required for continuous operation as shown in Figure 2.4a. In the case of rotary type regenerators, a portion of rotating matrix is exposed to hot fluid then to cold fluid thereby exchanging the heat gained from the hot fluid to cold fluid. Figure 2.4b shows the rotary regenerator.

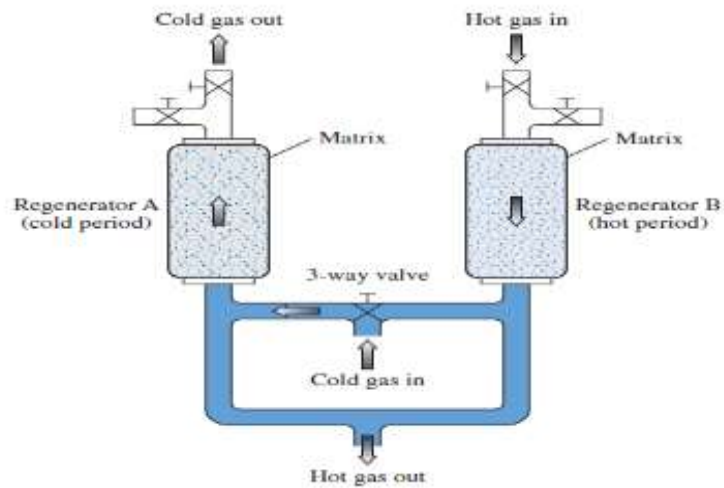


Figure 2.4a: Fixed dual-bed regenerator (Frank, 2011)

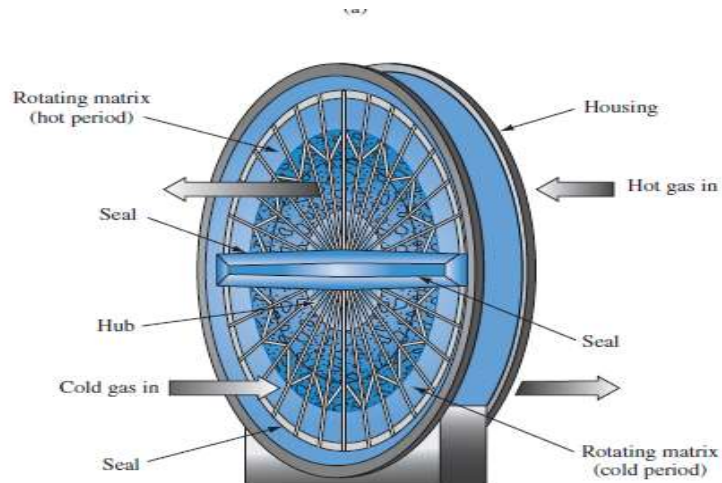


Figure 2.4b: Rotary regenerator (Frank, 2011)

2.2.2 Heat transfer process:

Based on the heat transfer process heat exchangers are classified direct and indirect contact types. The direct contact type. Heat transfer occurs at the interface between the hot and cold fluid, there is no separating wall between the hot and cold fluids. The fluid streams in direct contact can be two immiscible liquids gas- liquid pairs or a solid particle- fluids combination. Heat and mass transfer between the two fluids occur simultaneously, Some examples of direct contact type heat exchangers are cooling towers, spray and tray condenser. For the indirect type heat exchangers, the heat is exchanged between two fluids through a partition wall between the hot and cold fluids, the two fluids exchanges heat while flowing simultaneously (Kakas and Liu, 2002).

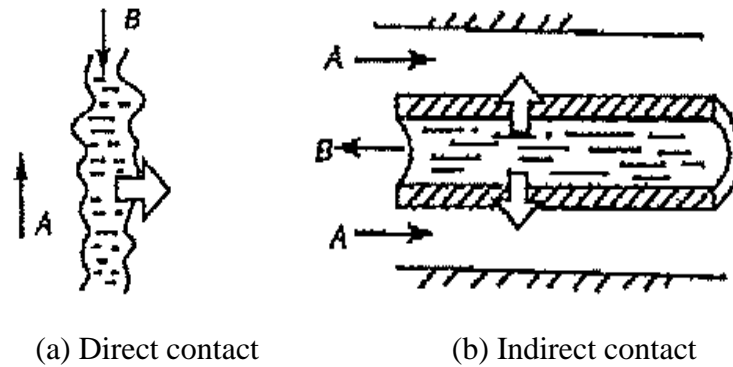


Figure 2.5: Type heat exchangers based on heat transfer process

2.2.3 The geometry of constructions

The main construction types of heat exchangers are tubular, plates and extended surfaces heat exchangers. The tubular type consists of circular tubes, one fluid flow through the inner tube and the other through the outer tube or annulus. The number of tubes, pitch of the tubes, tubes length and arrangement can be selected based on the required design, its further classified as double pipe, shell and tubes and spiral tube heat exchangers.

The plate type heat exchangers consist of thin plates forming flow channels, the fluid streams are separated by flat plates which are smooth between corrugated fins, mostly the plate types heat exchangers are used for heat transfer for any combination of liquids, gas, and two phase streams, and can be further classified as gasketed, spiral plates and lamella type. Lastly, the extended surface type heat exchangers are devices with fins on the main heat transfer surface, aimed to increases the heat transfer area. Finned surfaces are mostly used on the gas side to increase the heat transfer area as the heat transfer coefficients of the gas are lower compared with that of liquids (Kakas and Liu, 2002).

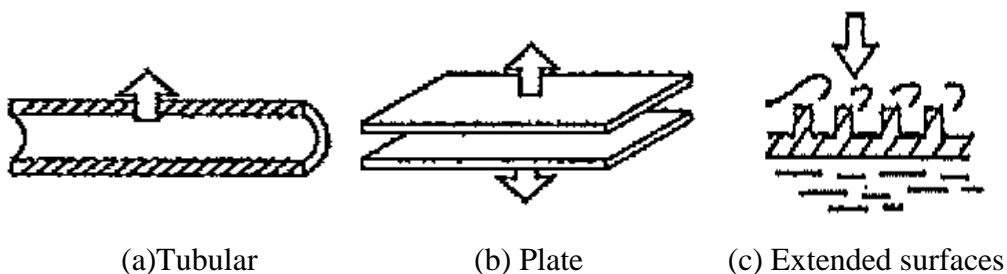


Figure 2.6: Types of heat exchangers based on geometry of construction

2.2.4 Heat transfer mechanism

The heat exchangers can be classified based on the heat transfer mechanism as,

- a. Single phase convection on both side: A single phase convection type includes economizers, boilers, air heaters, compressors in which single-phase convection occur on both sides.
- b. Single- phase convection one side and two-phase convection on another side: Heat exchanger devices used in pressurized water reactor such as a condenser, boilers, steam generators has condensation or evaporation on one of its sides.
- c. Two-phase convection on both sides: in this case, both sides of the exchanger undergoes two phase heat transfer such as condensation and evaporation (Kakas and Liu, 2002).

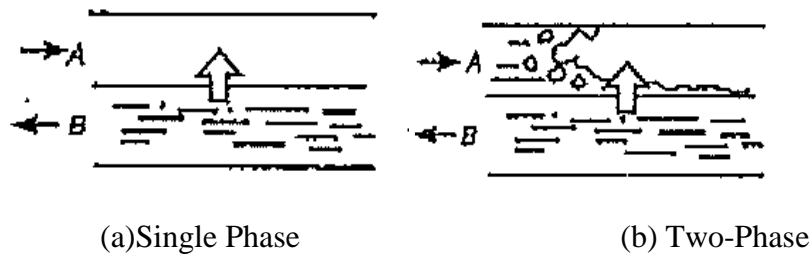


Figure 2.7: Heat exchangers based on mechanism of heat transfer

2.2.5 Flow arrangements

Heat exchangers are classified based on the direction of fluids flow arrangement as Parallel, Counterflow and cross flow types. In parallel flow, the two fluids streams flow in the same direction as shown in Figure 2.8a, the fluids enter and leave at one end. For counter flow exchanger the fluids flow in opposite direction, a typical counter flow exchanger is shown in Figure 2.8b in which the two fluid enters and exit at different ends. Finally, the cross flow type one fluid flows through the heat transfer surface at a right angle to the flow path of the other fluid. The two fluids flow could be mixed or unmixed (Kakas and Liu, 2002).

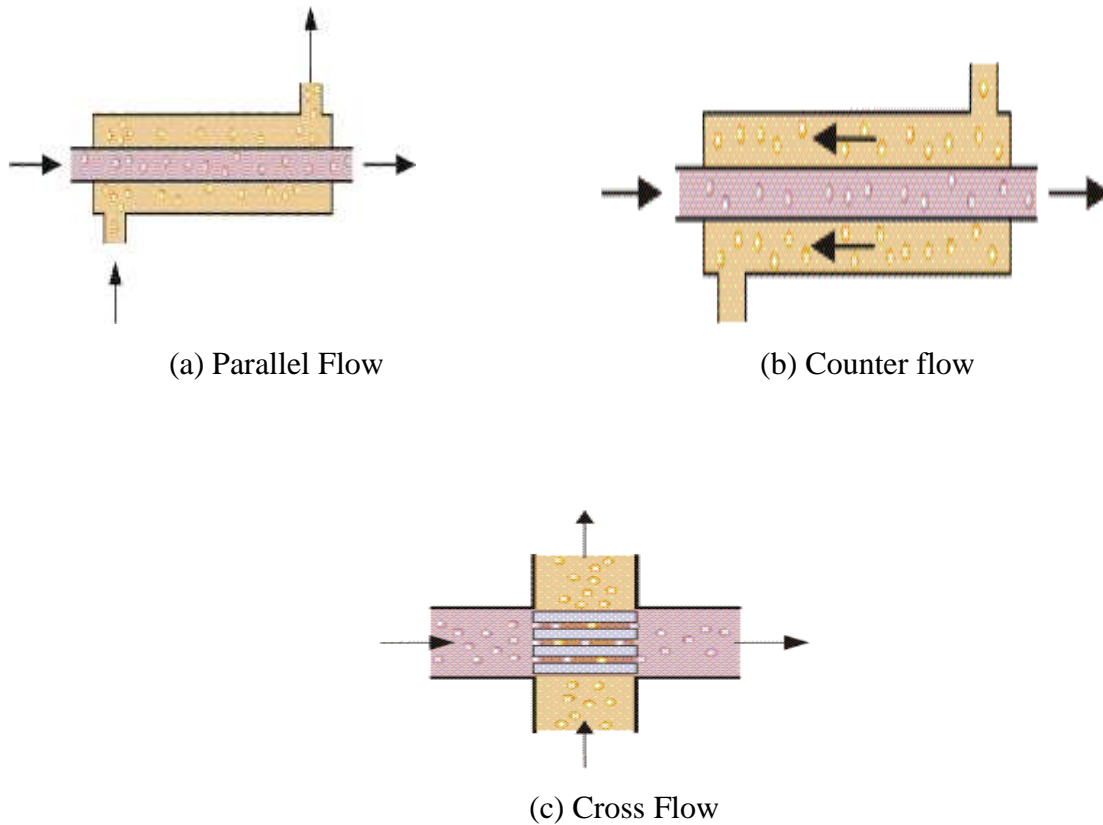


Figure. 2.8: Heat Exchangers Classification based on flow arrangement

2.3 Overall Heat Transfer Coefficient (U)

The overall heat transfer coefficient of exchanger is defined as total thermal heat transfer resistance between two fluids, it's determined by conduction and convection resistances of the fluids and the separating plane or cylindrical wall, given by

$$\frac{1}{UA} = \frac{1}{(UA)_c} = \frac{1}{(UA)_h} = \frac{1}{(hA)_c} + R_w + \frac{1}{(hA)_h} \quad (2.15)$$

Where index c and h refers to cold and hot fluids.

In determination of UA, since $(UA)_c = (UA)_h$ designation of hot or cold fluid is not required. The evaluation of overall coefficient depends on which surface area of the exchanger it's based on, which can be either cold or hot fluid side surface area, since $U_c \neq U_h$ if $A_c \neq A_h$.

The conduction resistance R_w for plane wall is defined as the ratio of driving potential to the heat transfer rate. Consider a heat transfer through a plane wall with thickness L.

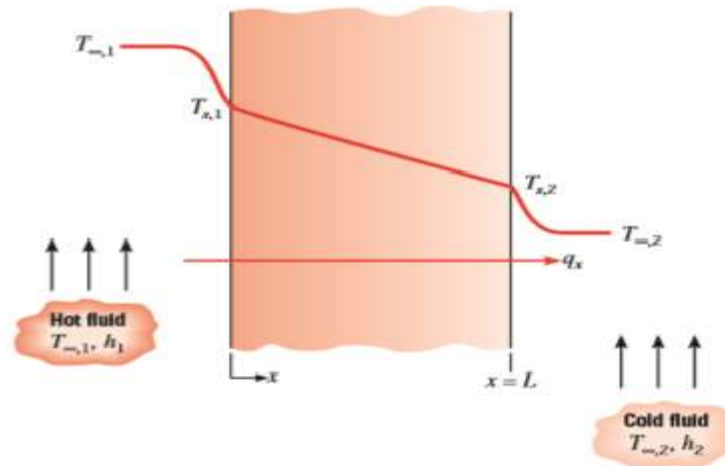


Figure 2.9: Heat Transfer Through a plane wall (Theodore et al., 2002)

The conduction resistance is expressed as,

$$R_{cond} = \frac{T_{S1} - T_{S2}}{q_x} = \frac{L}{kA}$$

Consider a heat transfer through a hollow cylinder with length L and radii r_1 and r_2 below,

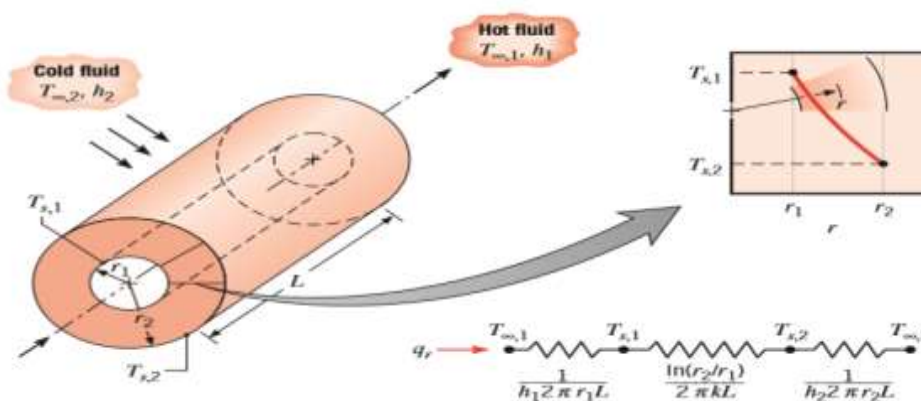


Figure 2.10: Hollow cylinder with the convective surface condition

The conduction resistance R_{cond}

$$R_{cond} = \frac{\ln(r_2/r_1)}{2\pi Lk}$$

The Equation 2.15, above is for clean and unfinned exchanger surfaces. Mostly the surfaces of the heat exchanger are subjected to fouling, rust and other reactions by the fluids in contact. The heat transfer resistances between two fluids increases as a result of scale or film deposition on the exchanger surfaces which can be treated by introducing additional thermal

resistance called fouling factor R_f that depends on operating temperature, velocity of the fluids and length of the exchanger. (Kakas and Liu, 2002).

For extended surface heat exchanger, the increase in surface area effect the overall heat transfer resistance, the modified overall heat transfer coefficient that includes fouling and fins effect is given by, (Theodore, et al., 2002).

$$\frac{1}{UA} = \frac{1}{(\eta_o hA)_c} + \frac{R_{fc}}{(\eta_o A)_c} + R_w + \frac{R_{fh}}{(\eta_o A)_h} + \frac{1}{(\eta_o hA)_h} \quad (2.16)$$

The fouling factors are obtained from fouling factor tables for different types of fluid and operating temperatures. The finned surface efficiency or temperature effectiveness η_o is defined based on the rate of heat transfer equation for hot or cold fluid without fouling as,

$$\dot{Q} = \eta_o hA(T_s - T_\infty)$$

Where,

T_s is surface temperature.

A is the total surface area (exposed base plus fin),

The surface efficiency η_o is defined as

$$\eta_o = 1 - \frac{A_f}{A}(1 - \eta_f)$$

Fin surface area A_f and the efficiency of single fin η_f is defined for straight or pin fin with adiabatic tip and length L as,

$$\eta_f = \frac{\tanh(mL)}{mL}$$

Where $m = \left(2h/kt\right)^{1/2}$ and t represent fin thickness.

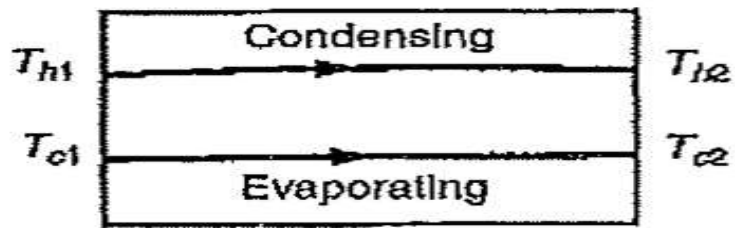
Conclusively, the overall heat transfer coefficient can be determined from convection coefficients, a fouling factor of hot and cold fluid and the exchanger geometric parameters. For unfinned surface exchanger, the convection coefficient can be determined from convection correlations and for finned surfaces from Kays and Landon table of the convective coefficient (Theodore et al., 2002).

2.3.1 Variable overall heat transfer coefficient

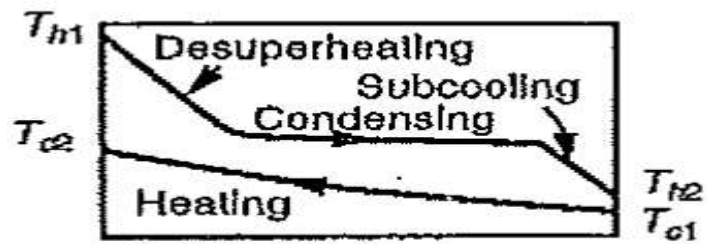
The overall heat transfer coefficient cannot be constant throughout the exchanger, its value varies along the exchanger. The overall heat transfer coefficients of exchanger depend on the flow Reynolds number, the geometry of heat transfer surface and the physical properties of the fluids. The method to account of its variations is given for particular exchanger type (Theodore et al., 2002)

Consider the following cases of the heat exchanger with variable overall coefficients as shown in Figure 2.11. For a case in Figure 2.11a, both fluids undergo phase changes with no sensible heating or cooling, at constant temperatures. Figure 2.11b, shows a case where one fluid vapor with a temperature above saturation temperature is condensed to sub-cooled before exiting the condenser and opposite of the case is true for Figure 2.11c, where a subcooled fluid is heated to superheat. When the hot fluid consists of a mixture of condensable and non-condensable gases it results in complex temperature distribution as shown in Figure 2.11d.

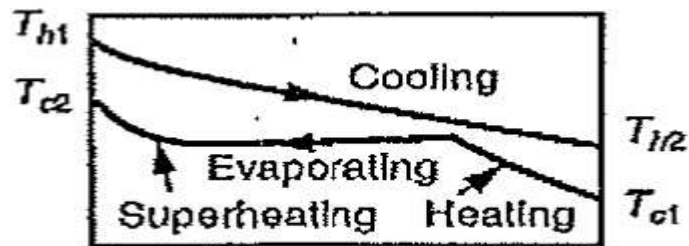
The most difficult approach in the design of heat exchanger is when the overall heat transfer coefficient varies continuously with a position in the exchanger. Consider Figure 2.11b and Figure 2.11c, in which the exchanger has three parts with a constant value of U , for this case, it's treated as three different exchangers in series. Generally, for heat exchanger with variable overall heat transfer coefficient, it's divided into segments based on the value of overall heat transfer coefficient designated to each segment. The analysis could be done numerically or using finite difference method (Kakas and Liu, 2002).



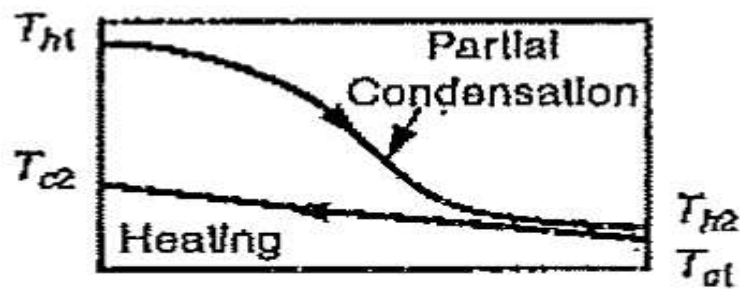
(a) Both fluids changing phase



(b) One fluid changing phase



(c) One fluid changing phase



(d) Condensable and Non-condensable component

Figure 2.11: Typical cases of the heat exchanger with variable overall coefficient

2.4. Heat Exchanger Design Methods

The main problems in the design of heat exchangers are rating and sizing. The rating problem concerned with the determination of heat transfer rate and the fluid outlet temperatures for prescribed flow rates, inlet temperatures and allowable pressure drop for a heat exchanger. The sizing problems deal with the determination of heat exchanger dimensions to meet the required hot and cold fluids inlets and outlet temperatures conditions (Kakas and Liu, 2002). For performance analysis of heat exchangers, it is necessary to relate the total rate heat transfer to the inlet and outlet fluids temperatures, the overall heat transfer coefficient and the total heat transfer area. This relation could be obtained by applying overall energy balance on hot and cold fluids, as shown in Figure 2.12.

If \dot{Q} represent the rate of heat transfer between the two fluids, by applying the steady flow energy equation with negligible changes in kinetic and potential energy and no heat is transferred with surrounding, we obtained

$$\dot{Q} = \dot{m}_h(i_{hi} - i_{ho}) = \dot{m}_c(i_{co} - i_{ci}) \quad (2.17)$$

Where,

i_h and i_c represent enthalpy for hot and cold fluids.

For constant specific heat and the fluids do not undergo phase changes, Equation 2.17 reduced to

$$\dot{Q} = \dot{m}_h c_{ph}(T_{hi} - T_{ho}) = \dot{m}_c c_{pc}(T_{co} - T_{ci}) \quad (2.18)$$

The temperature at a specified location is represented by mean value. It can be observed that Equation 2.18 is independent of types of heat exchangers and flow arrangements (Theodore et al., 2002). Using Newton's law of cooling another useful relationship is obtained by relating the total heat transfer \dot{Q} to the temperatures difference between the hot and cold fluid ΔT , and the overall heat transfer coefficient U , since ΔT changes with position in the heat exchanger, then heat transfer rate is given by,

$$\dot{Q} = UA\Delta T_m \quad (2.19)$$

Where,

ΔT_m represent the mean temperature difference.

2.4.1 Logarithmic mean temperature method (LMTD)

The temperatures of cold and hot fluids changes with the position when flowing through an exchanger and the rate of heat transfer depend on the temperature difference between the between the hot and cold fluids involved (Frank, et. al, 2011).

The LMTD is used in design analysis when the fluids flow rates, inlet temperatures and desired outlet temperature of the fluid are prescribed for a particular exchanger type. For performance analysis in determination of outlet temperatures iterative method can be used for given inlet temperature.

Consider a parallel and counter flow heat exchangers below,

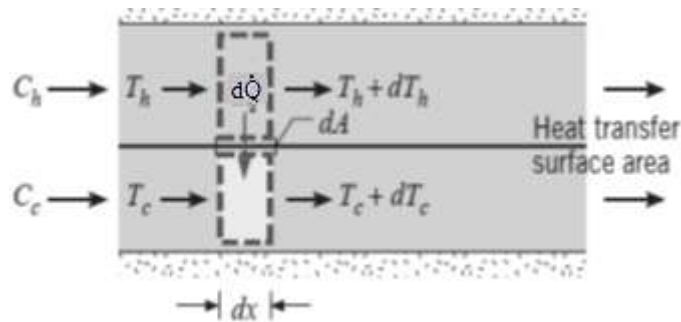


Figure 2.12: Energy balance for parallel flow heat exchangers (Augusto, 2013)

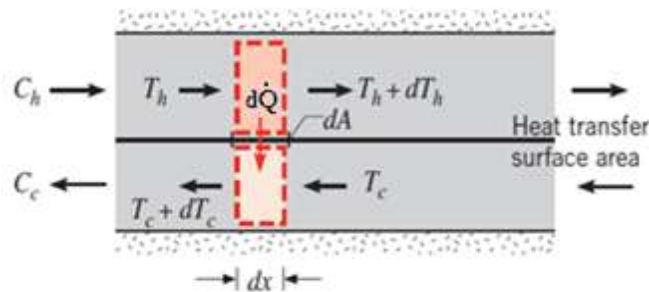


Figure 2.13: Energy balance for counter flow heats exchangers (Theodore et al., 2002)

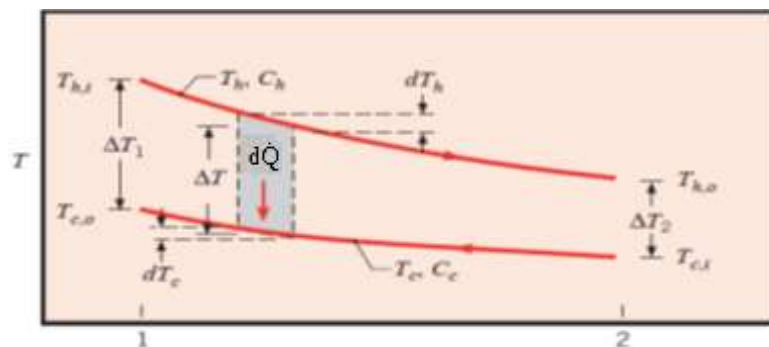


Figure 2.14: Temperature profile for counter flow heat exchanger (Theodore et al., 2002)

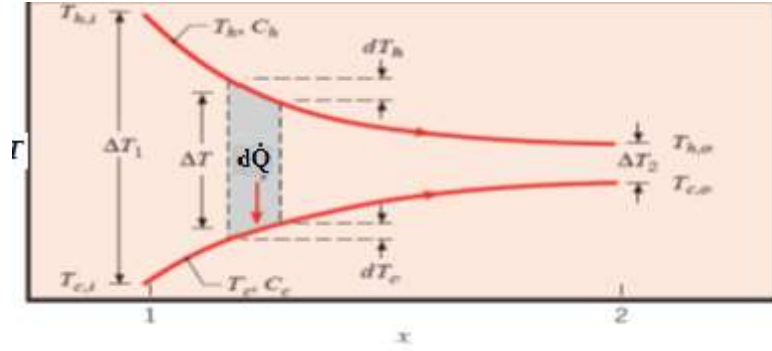


Figure 2.15: Temperature profile for parallel flow heat exchanger (Theodore et al., 2002).

The mean temperature is determined by applying energy balance on a differential element dA , of hot and cold fluids. For a parallel flow heat exchanger shown in Figure 2.15, the temperatures of the hot fluids drop by dT_h and that of cold fluid increase by dT_c while in Figure 2.14 of counter flow exchanger the temperature of the cold fluid drop by dT_c over the element dA .

For steady flow Equation, 2.17 is transformed to

$$d\dot{Q} = -C_h dT_h = \pm C_c dT_c \quad (2.20)$$

Where,

C_h and C_c are the specific heat capacity rates of hot and cold fluids. The positive sign for parallel flow and the negative for counter flow heat exchangers.

The local heat transfer between the fluids is given by

$$d\dot{Q} = U dA \Delta T \quad (2.21)$$

Where the ΔT is local temperature difference, expressed as,

$$d(\Delta T) = dT_h - dT_c \quad (2.22)$$

Substituting Equation 2.20 into Equation 2.21, integrating and simplifying result in

$$\dot{Q} = UA \frac{\Delta T_2 - \Delta T_1}{\ln \frac{\Delta T_2}{\Delta T_1}} = UA \Delta T_{LMTD} \quad (2.23)$$

The term $\frac{\Delta T_2 - \Delta T_1}{\ln \frac{\Delta T_2}{\Delta T_1}}$ is called the log. mean temperature difference ΔT_{LMTD} .

Where,

$$\Delta T_1 = (\Delta T_{h1} - \Delta T_{c1}) \text{ and } \Delta T_2 = (\Delta T_{h2} - \Delta T_{c2}), \text{ for parallel flow heat exchangers}$$

$$\Delta T_1 = (\Delta T_{hi} - \Delta T_{co}), \text{ and } \Delta T_2 = (\Delta T_{ho} - \Delta T_{ci}), \text{ for counter flow heat exchangers.}$$

2.4.2 Multipass and cross flow heat exchanger

A concept of corrected LMTD method is used in the analysis of multi-pass and cross flow heat exchanger as the previous LMTD method not applicable to multi-pass and cross flows heat exchangers. The rate of heat transfer from hot to cold fluid across a surface area dA of heat exchanger is expressed as

$$d\dot{Q} = U(T_h - T_c)dA$$

For multi-pass and cross flow arrangement, integrating the above equation gives the rate of heat transfer in term of integrated temperature difference as,

$$\dot{Q} = UA\Delta T_m \quad (2.26)$$

The ΔT_m in Equation 2.26, refers to effective mean temperature difference that can be determined analytically. For a design purposes of multi-pass and cross flow heat exchanger the ΔT_m is modified by introducing a dimensionless factor F which depends on temperature effectiveness P and ratio of heat capacity rate R.

$$F = \phi(P, R, \text{Flow arrangement})$$

$$Q = UAF\Delta T_{lmcf}$$

Where the,

$$R = \frac{T_{c2} - T_{c1}}{T_{h1} - T_{c1}} = \frac{C_c}{C_h} \quad \text{and} \quad P = \frac{T_{c2} - T_{c1}}{T_{h1} - T_{c1}} = \frac{\Delta T_c}{\Delta T_{max}}$$

The correction factor F is the measure of degree of deviation of effective mean temperature ΔT_m from log mean temperature difference (LMTD). F is less than one for multi pass and cross flow arrangement and equal to one for perfect counter flow heat exchanger.

A chart of correction factor F values was prepared by Bowman et al in 1940 for multipass shell and tube and cross flows heat exchangers and it's available in many heat transfer textbooks.

Except if the fluids in multi-pass or cross flow are well mixed along the flow path the fluid temperature is not uniform at a specific location of the exchanger. Series of baffles are employed to properly mix the fluids. Some of the correction factors F charts for three two shell pass and unmixed cross flows heat exchangers are present below,

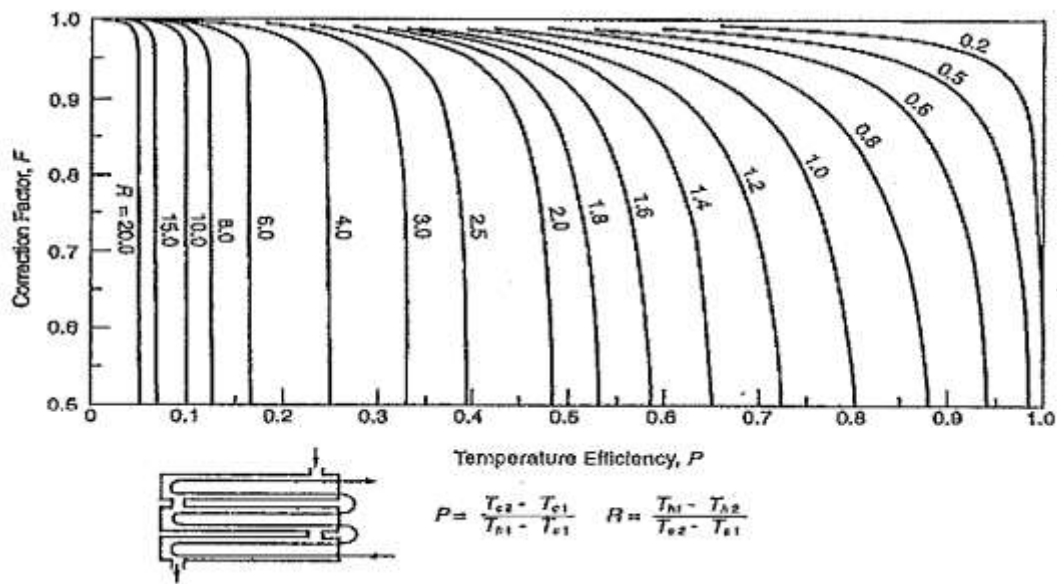


Figure 16: Correction factor F for the shell and tube type with the three and two shell passes and six either more even numbers of passes (Kakas and Liu, 2002)

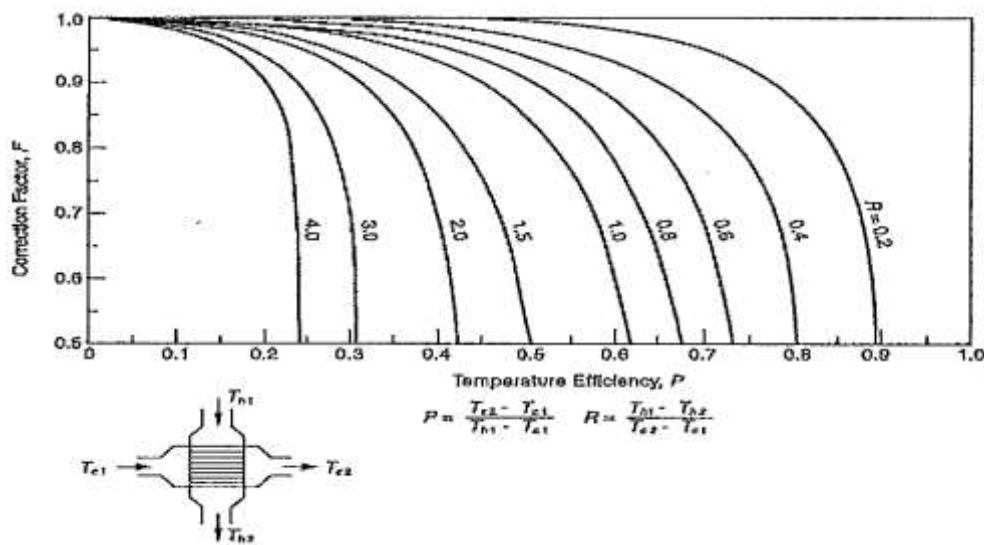


Figure 17: Correction factor F for cross flow heat exchanger with both fluid unmixed

2.4.3 Effectiveness-NTU method

The concept of the ϵ -NTU method was first introduced by London and Seban in 1942. The method was used in 1952 by Kays and London in formulation of data for different geometries and flow arrangements of compact heat exchanger, and since then it's considered as the most accepted method for design and analysis of heat exchangers (London and Seban, 1980).

The previous LMTD method developed is only applicable when the inlets and outlets temperatures of the fluids are known. The effectiveness-NTU method is focused mainly on the concept of maximum possible heat transfer rate could be used when only inlet temperatures are known. In this method, one of the fluids would achieve maximum temperatures difference of ΔT_{max} in a finite length of counter flow heat exchangers (John, 2001).

The rate of heat transfer from hot to cold fluid in the exchanger is

$$\dot{Q} = C_{min}(T_{hi} - T_{ci}) = \varepsilon C_{min} \Delta T_{max} \quad (2.27)$$

Where,

ε is the effectiveness of the exchanger, and C_{min} is minimum capacity rate.

The effectiveness of heat exchanger depends on number of transfer unit (NTU), heat capacity ratio (C^*) and flow arrangement.

$$\varepsilon = \phi(NTU, C^*, \text{flow arrangement})$$

2.4.4 Heat Exchanger Effectiveness

The effectiveness(ε) is used to measure the performance of a heat exchanger, defined as the ratio of the actual rate of heat transfer from hot to the cold fluid to the thermodynamically permitted maximum heat transfer rate (Shah and Sekulic, 2003).

$$\varepsilon = \frac{\dot{Q}}{\dot{Q}_{max}} \quad (2.28)$$

Consider a counter flow heat exchanger in Figure 2.14, for infinite surface area the overall energy balance of hot and cold fluid streams is expressed as

$$\dot{Q} = C_h(T_{hi} - T_{ho}) = C_c(T_{co} - T_{ci}) \quad (2.29)$$

In Equation 2.29, for $C_h < C_c$, that is $(T_{hi} - T_{ho}) > (T_{co} - T_{ci})$ the maximum temperature difference occur in the hot fluid, then over infinite flow length of the exchanger the exit temperature of hot fluid approaches the inlet temperature of cold fluid ($T_{ho} = T_{ci}$) as shown in Figure 2.18. Hence, for infinite counter flow heat exchanger with $C_h < C_c$, the maximum heat transfer is given by

$$\dot{Q}_{max} = C_h(T_{hi} - T_{ci}) = C_h \Delta T_{max} \quad (2.30)$$

Likewise, for the case whereby $C_h = C_c = C$,

$$\dot{Q}_{max} = C_h(T_{hi} - T_{ci}) = C_c(T_{hi} - T_{ci}) = C \Delta T_{max} \quad (2.31)$$

Finally, for $C_c < C_h$, $(T_{co} - T_{ci}) > (T_{hi} - T_{ho})$, and from Figure 2.18 the outlet temperature of cold fluid approaches the inlet temperature of hot fluid, over infinite length of the exchanger.

$$\dot{Q}_{max} = C_c(T_{hi} - T_{ci}) = C_h\Delta T_{max} \quad (2.32)$$

Generally, the maximum heat transfer rate considering the above cases is given by,

$$\dot{Q}_{max} = C_{min}(T_{hi} - T_{ci}) = C_{min}\Delta T_{max} \quad (2.33)$$

Where,

$$C_{min} = \begin{cases} C_c & \text{for } C_h > C_c \\ C_h & \text{for } C_h < C_c \end{cases}$$

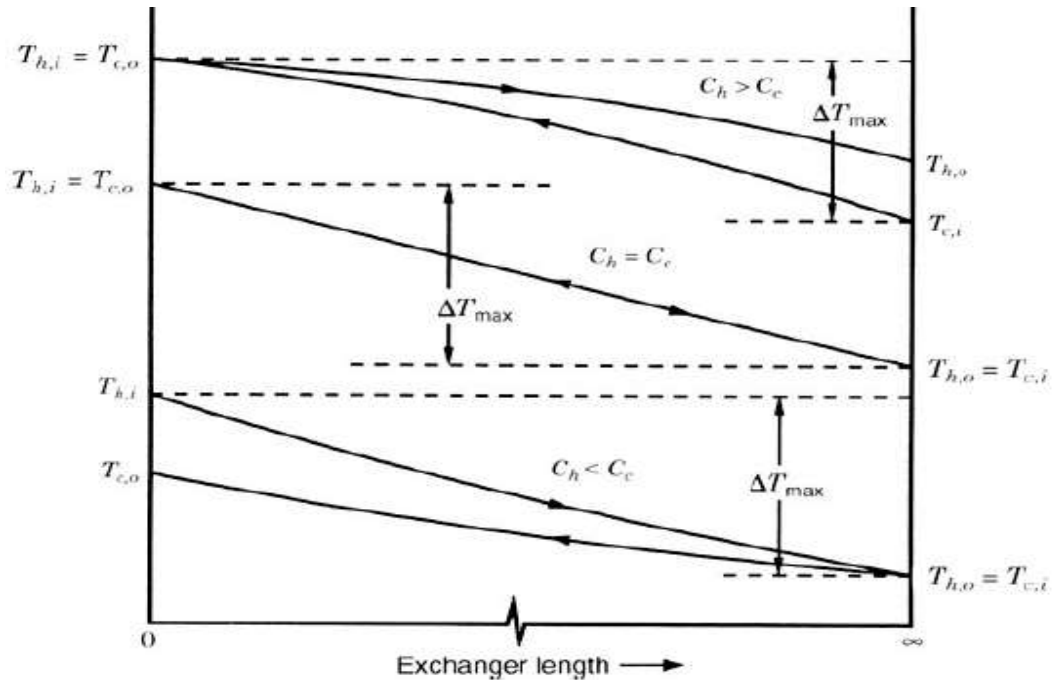


Figure 2.18: Temperature distribution in counter flows heat exchanger of the infinite area

The effectiveness of an exchanger is

$$\varepsilon = \frac{\dot{Q}}{\dot{Q}_{max}} = \frac{C_h(T_{hi} - T_{ho})}{C_{min}(T_{hi} - T_{ci})} = \frac{C_c(T_{co} - T_{ci})}{C_{min}(T_{hi} - T_{ci})} \quad (2.34)$$

It can be seen that the effectiveness can be determined directly from the exchanger operating temperatures, and the expression for effectiveness can also be expressed as, (Shah and Sekulic, 2003).

$$\varepsilon = \frac{UA}{C_{min}} \frac{\Delta T_m}{\Delta T_{max}} \quad (2.35)$$

The two dimensionless parameters, the number of transfer unit (NTU) and average temperatures difference θ are introduced to characterize a heat exchanger (Theodore, et al. 2002).

$$\theta = \frac{\Delta T_{LM}}{T_{hi} - T_{ci}} \quad \text{and} \quad NTU = \frac{UA}{C_{min}} = \int_A U dA$$

The dimensionless parameter NTU is a measure of the thermal length of the heat exchangers. It can be seen that the effectiveness is a function of NTU and the capacity ratio C^* . The charts of effectiveness against NTU are developed for the analysis of various types of heat exchangers. Below are some of the $\varepsilon - NTU$ charts,

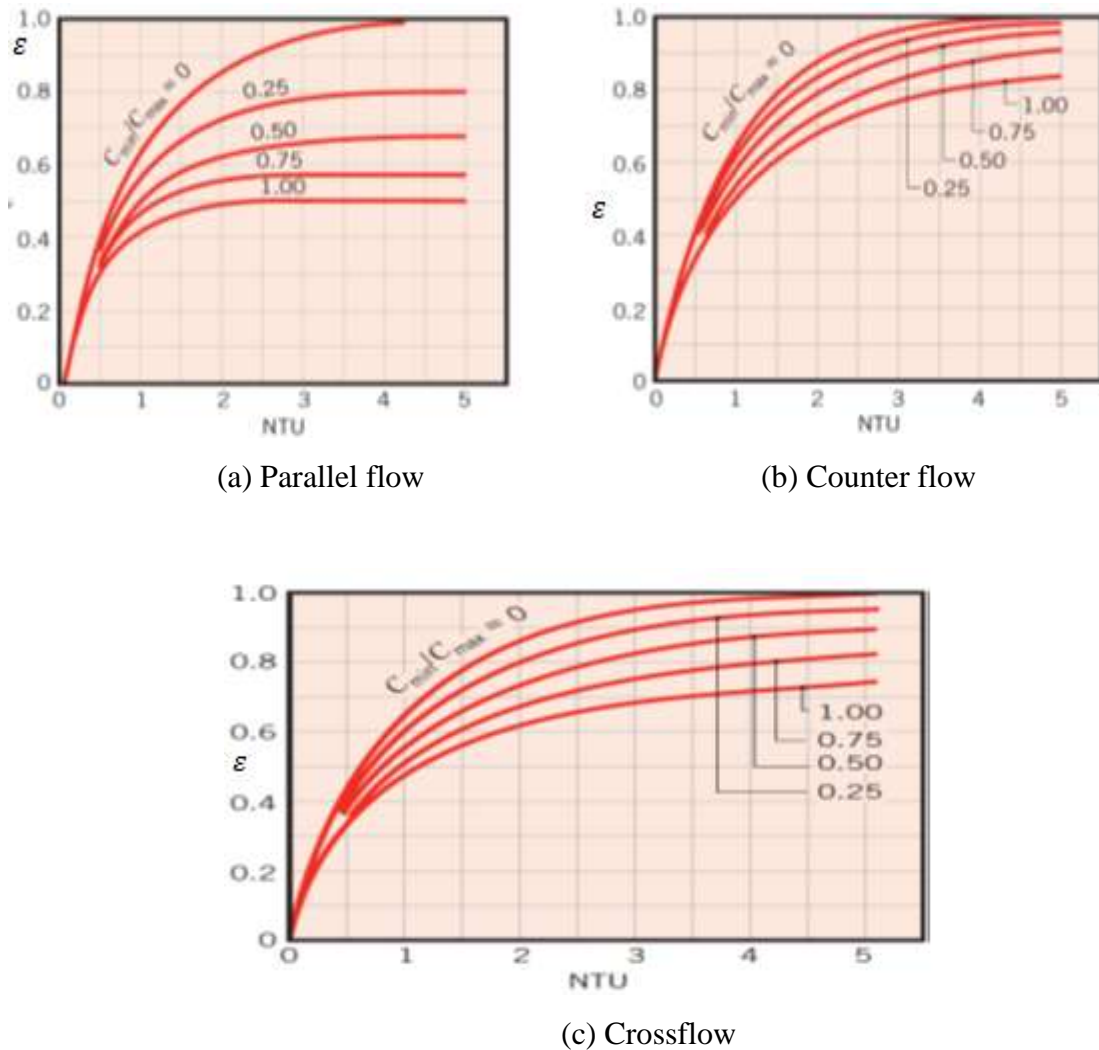


Figure 2.19: Effectiveness-NTU charts of heat exchangers (Theodore et al. 2002)

2.4.5 Heat capacity ratio (C^*)

The heat capacity ratio is defined as the ratio of minimum to the maximum capacity ratio such that $C^* \leq 1$. A heat exchanger is balanced when the two fluids has equal capacity ratios are ($C^* = 1$). (Shah and Sekulic, 2003).

$$C^* = \frac{C_{min}}{C_{max}}$$

$C^* = 0$ Corresponds to a case in with finite C_{min} and the C_{max} approaching ∞ (condensing and evaporating fluids) (Kays and London, 1984).

2.5 Heat Transfer Dimensionless Numbers

2.5.1 Nusselt number (Nu):

Nu is a dimensionless number named after German Engineer Wilhelm Nusselt. According to Shah, 2003, it's defined as the ratio of convective conductance (h) to the thermal conductance (K/D_h) of pure molecules. And it's dimensionless representation of heat transfer coefficients. Nusselt number may be represented as a ratio of convection to conduction heat transfer.

$$Nu = \frac{hD_h}{k} = \frac{\dot{q}D_h}{k(T_w - T_m)} \quad (2.36)$$

Where \dot{q} heat transfer per unit area, T_w and T_m are wall and mean temperatures as shown in Figure 2.20. The physical significance of Nusselt number in thermal circuit was that the convective coefficient h in Nu represent convective conductance, the heat flux as current and $(T_w - T_M)$ as potential.

For laminar flow, the Nusselt number depend strongly on thermal boundary conditions and geometry of flow passage while in the turbulent flow it's weakly dependent on these parameters. Nusselt number is constant for thermally and hydrodynamically fully developed laminar flow and for developing laminar temperature and velocity profile depend on dimensional axial heat transfer length $x^* = x/D_h P_e$ and Prandtl number (Pr). For the case of fully developed turbulent flow the Nusselt number depend on Reynold number (Re), Pr, thermal boundary conditions, geometry of flow passage and flow regimes it's also dependent on phase condition (Shah and Sekulic, 2003).

2.5.2 Prandtl number (Pr)

A dimensionless number named after German physicist Ludwig Prandtl is defined as the ratio of momentum diffusivity to the thermal diffusivity of the fluids.

$$Pr = \frac{\nu}{\alpha} = \frac{\mu C_p}{k} \quad (2.38)$$

The Prandtl number is entirely fluid properties and it has ranges of values as 0.001 to 0.03 for liquid metals, 0.2 to 1 for gas, 1 to 13 for water, 5 to 50 for light organic liquids, 50 to 10^5 for oils and lastly 20000 to 10^5 for glycerin (Shah and Sekulic, 2003).

2.5.3 Stanton Number

The heat transfer coefficient is also represented in terms of a dimensionless number called Stanton number (St), named after Thomas Edward Stanton (1865- 1931). It's defined as the ratio of convected heat transfer per unit surface area to the rate of enthalpy change of the fluid reaching the wall temperature per unit cross-sectional area of the flow.

$$St = \frac{h}{GC_p} = \frac{h}{\rho U_m C_p} \quad (2.39)$$

For single phase fluid, the relationship between rate of enthalpy change to heat transfer from fluid to the wall or in opposite case is given by,

$$hA(T_w - T_m) = A_o GC_p (T_o - T_i) = GC_p A_o \Delta T \quad (2.40)$$

$$St = \frac{h}{GC_p} = \frac{A_o \Delta T}{\Delta T_m} \quad (2.41)$$

Where, $\Delta T_m = T_w - T_m$,

From the above Equation 2.41, it can be seen that the Stanton number is proportional to the change fluid temperature divided by driving potential of convection heat transfer. Stanton number is preferred frequently to Nusselt number (Nu) for correlation of convective heat transfer when axial heat conduction is negligible. Stanton number is directly related to number of transfer unit (NTU) as

$$St = \frac{h}{GC_p} = \frac{hA}{mC_p} \cdot \frac{A_o}{A} = ntu \frac{\Delta h}{4L} \quad (2.42)$$

Also, the Stanton, Prandtl, Reynolds numbers are related to Nusselt number as

$$Nu = St Re Pr \quad (2.43)$$

This shows Stanton number is irrespective of boundary condition, the geometry of flow passage and types of flow (Shah and Sekulic, 2003).

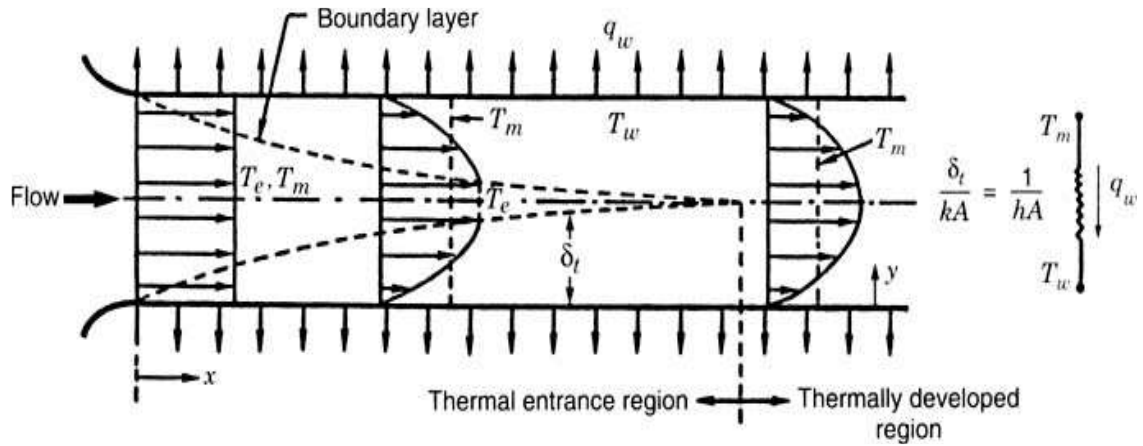


Figure 2.20: Laminar thermal boundary layer in a tube (Shah and Sekulic, 2003).

2.5.4 Number of transfer unit (NTU)

NTU is a dimensionless design parameter defined as the ratio of overall thermal conductance to the minimum heat capacity rate. It represents the heat transfer size of an exchanger.

$$NTU = \frac{UA}{C_{min}} = \frac{1}{C_{min}} \int_A U dA \quad (2.44)$$

For variable overall heat transfer coefficient, U the NTU is evaluated using the last term of Equation 2.44. For small capacity rate fluid NTU is represented as the relative magnitude of heat transfer rate in contrast with the rate of enthalpy change. The product of overall heat transfer coefficient U and surface area provide a measure of heat exchanger size. The NTU does not necessarily represent the physical size of the exchanger, in contrast, the heat transfer surface area represents the heat exchanger physical size. For specific application of heat exchanger $\frac{U}{C_{min}}$ is approximately kept constant. High value of NTU can be attained by either increasing U or A or both or by decreasing the minimum capacity rate. NTU and overall Stanton number are related directly with U in the form

$$NTU = St_o \frac{4L}{D_h} \quad (2.45)$$

Where D_h is hydraulic diameter (Shah and Sekulic, 2003).

CHAPTER 3

GOVERNING EQUATIONS AND BOUNDARY CONDITIONS

3.1 Governing Equations and Boundary Conditions

3.1.1 Governing equations

Consider a section of bayonet tube heat exchanger differential control volume below,

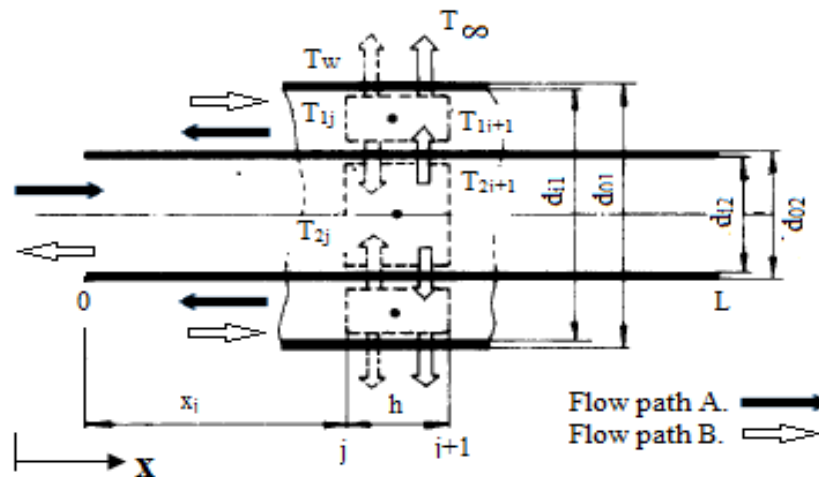


Figure. 3.1: The energy balance of bayonet tube heat exchanger section

Assumptions

- Steady and fully developed flow is assumed,
- The axial heat conduction is neglected.
- The fluids temperatures are represented by the mean values at a particular cross-section. Inner and outer tubes fluids temperatures are assumed to be equally at bayonet tube end ($x = L$), thus the heat transfer at that particular cross-section is negligible.
- The overall heat transfer coefficients U_2 between the inner tube and the annulus which is assumed to be constant along the flow direction.
- The overall heat transfer coefficient U_1 between the annulus fluid and outer surface is assumed to be uniform for the entire flow length of exchanger
- The outer tube surface wall temperature T_w is assumed to be constant for the exchanger flow length.

Taking the energy balance on the differential control volume in Figure 3.1,

$$\left[\begin{array}{c} \text{Energy entering} \\ \text{with fluids} \end{array} \right] - \left[\begin{array}{c} \text{Energy of the} \\ \text{leaving} \\ \text{leaving fluids} \end{array} \right] - \left[\begin{array}{c} \text{Heat transfer} \\ \text{by the leaving fluid} \end{array} \right] = \left[\begin{array}{c} \text{Energy stored} \\ \text{in the fluid} \end{array} \right]$$

For inner tube,

$$\dot{m}C_p \frac{dT_2}{dx} \pm U_2p_2(T_2 - T_1) = 0 \quad (3.1)$$

And for annulus

$$\dot{m}C_p \frac{dT_1}{dx} \pm [U_2p_2(T_2 - T_1) - U_1p_1(T_1 - T_w)] = 0 \quad (3.2)$$

The plus and minus sign (\pm) represent the energy balance for flow arrangements A and B respectively.

3.1.2 The boundary conditions

At inlet condition of the flow arrangement A and exit of flow arrangement B.

$$x = 0 \quad T_z = T_{in} \quad (3.3)$$

At bayonet tube sealed end

$$x = L \quad T_1 = T_2 \quad (3.4)$$

Where the subscript z is 2 for path A and 1 for path B,

3.1.3 Non-dimensionalization

The temperature differential Equations 3.1 and 3.2 are transformed to dimensionless form by introducing the following dimensionless parameters,

Dimensionless inner tube fluid temperature θ_2

$$\theta_2 = \frac{T_2 - T_w}{T_{in} - T_w}$$

Dimensionless annulus fluid temperature θ_1

$$\theta_1 = \frac{T_1 - T_w}{T_{in} - T_w}$$

The dimensionless exchanger flow length X

$$X = \frac{h_{o1}P_{o1}}{\dot{m}C_p} x$$

The dimensionless flow length X is equivalent to local number of transfer unit (NTU_x).

differentiating the above dimensionless parameters for constant wall temperature T_w ,

$$\frac{dT_1}{dx} = (T_{in} - T_w) \frac{d\theta_1}{dx} \quad (3.5)$$

$$\frac{dT_2}{dx} = (T_{in} - T_w) \frac{d\theta_2}{dx} \quad (3.6)$$

$$\frac{dX}{dx} = \frac{h_{o1}P_{o1}}{mC_p} \quad (3.7)$$

For inner tube,

Transforming Equation 3.1 through Equation 3.6 gives

$$(T_{in} - T_w) \frac{d\theta_2}{dx} \pm \left[\frac{U_2 p_2}{\dot{m} C_p} (\theta_2 - \theta_1) \right] (T_{in} - T_w) = 0$$

$$\frac{d\theta_2}{dx} \pm \left[\frac{U_2 p_2}{\dot{m} C_p} (\theta_2 - \theta_1) \right] = 0 \quad (3.8)$$

Using Equation 3.7 on Equation 3.8 results,

$$\frac{d\theta_2}{dX} \pm \left[\frac{U_2 p_2}{\dot{m} C_p} L \cdot \frac{\dot{m} C_p}{h_{o1} p_{o1} L} (\theta_2 - \theta_1) \right] = 0$$

$$\frac{d\theta_2}{dX} \pm [Hu(\theta_2 - \theta_1)] = 0 \quad (3.9)$$

Similarly, for annulus side of the bayonet tube

The annulus temperature differential Equation 3.1 is transformed using Equation 3.5 as

$$(T_{in} - T_w) \frac{d\theta_1}{dx} \pm \left[\frac{U_2 p_2}{\dot{m} C_p} (\theta_2 - \theta_1) - \frac{h_1 p_1}{\dot{m} C_p} \theta_1 \right] (T_{in} - T_w) = 0$$

$$\frac{d\theta_1}{dx} \pm \left[\frac{U_2 p_2}{\dot{m} C_p} (\theta_2 - \theta_1) - \frac{h_1 p_1}{\dot{m} C_p} \theta_1 \right] = 0 \quad (3.10)$$

Using dimensionless flow length Equation 3.7, the Equation 3.10 becomes

$$\frac{d\theta_1}{dX} \pm \left[\frac{U_2 p_2 L}{\dot{m} C_p} \cdot \frac{\dot{m} C_p}{h_{o1} p_{o1} L} (\theta_2 - \theta_1) - \theta_1 \left(\frac{h_1 p_1}{\dot{m} C_p} \cdot \frac{\dot{m} C_p}{h_{o1} p_{o1}} \right) \right] = 0$$

$$\frac{d\theta_1}{dX} \pm \left[\text{Hu}(\theta_2 - \theta_1) - \theta_1 \left(\frac{h_1 p_1}{h_{o1} p_{o1}} \right) \right] = 0 \quad (3.11)$$

Now considering the outer tube of the bayonet tube to be a thin walled tube, the ratio of the outside to the inside of outer tube diameter is approximated to unity.

$$\frac{p_1}{p_{o1}} = \frac{d_1}{d_{o1}} \sim 1$$

Also the ratio of convective coefficients of inside and outside surface of the outer tube to be ξ defined as

$$\xi = \frac{h_1}{h_{o1}}$$

Then Equation 3.11 becomes

$$\frac{d\theta_1}{dX} \pm [\text{Hu}(\theta_2 - \theta_1) - \xi \theta_1] = 0 \quad (3.12)$$

Therefore, the resultant dimensionless temperature differential equations for tubes temperatures θ_1 and θ_2 are given by Equations 3.9 and 3.12,

$$\frac{d\theta_2}{dX} \pm [\text{Hu}(\theta_2 - \theta_1)] = 0$$

$$\frac{d\theta_1}{dX} \pm [\text{Hu}(\theta_2 - \theta_1) - \xi \theta_1] = 0$$

Where the Hurd number (Hu) and ratio of the convective coefficient (ξ) are constant.

The Hu is defined as the ratio of number of transfer unit of inner tube (ntu) to that of annulus side (NTU),

$$\text{Hu} = \frac{\text{ntu}}{\text{NTU}} \quad (3.13)$$

The ntu and NTU are given by,

$$\text{ntu} = \frac{U_2 p_2 L}{\dot{m} C_p} = \frac{U_2 A_2}{\dot{m} C_p} \quad (3.14)$$

$$NTU = \frac{h_{o1}P_{o1}L}{\dot{m}C_p} = \frac{h_{o1}A_{o1}}{\dot{m}C_p} \quad (3.15)$$

The exchanger exit fluids temperature conditions are determined by taking the overall energy balance on outer surface of the bayonet tube as,

$$\dot{Q} = \dot{m}C_p(T_{in} - T_{ex}) = \int_{x=0}^L h_{o1}p_{o1}(T_w - T_{\infty})dx \quad (3.16)$$

$$\dot{m}C_p[(T_{in} - T_w) - (T_{ex} - T_w)] = \int_{x=0}^L h_{o1}p_{o1}[(T_{in} - T_{\infty}) - (T_{in} - T_w)]dx$$

$$\dot{m}C_p \left[1 - \frac{(T_{ex} - T_w)}{(T_{in} - T_w)} \right] = \int_{x=0}^L h_{o1}p_{o1}[(T_{in} - T_w) - (T_{in} - T_{\infty}) - (T_{in} - T_w)]dx$$

$$\dot{m}C_p \left[1 - \frac{(T_{ex} - T_w)}{(T_{in} - T_w)} \right] = \int_{x=0}^L h_{o1}p_{o1} \left[1 - \frac{(T_{in} - T_{\infty})}{(T_{in} - T_w)} - 1 \right] dx$$

$$\left[1 - \frac{(T_{ex} - T_w)}{(T_{in} - T_w)} \right] = - \int_{x=0}^L \frac{h_{o1}p_{o1}}{\dot{m}C_p} \left[\frac{(T_{in} - T_{\infty})}{(T_{in} - T_w)} \right] dx \quad (3.17)$$

The dimensionless fluids exit temperature θ_{ex} and the shell side fluid temperature θ_{∞} are define as,

$$\theta_{\infty} = \frac{T_{\infty} - T_w}{T_{in} - T_w} \quad (3.18)$$

$$\theta_{ex} = \frac{T_{ex} - T_w}{T_{in} - T_w} \quad (3.19)$$

Transforming Equation 3.17 to dimensionless form using Equations 3.7, 3.18 and 3.19 gives

$$1 - \theta_{ex} = \int_{X=0}^L \theta_{\infty} dX$$

$$\theta_{ex} = 1 - \int_{X=0}^L \theta_{\infty} dX \quad (3.20)$$

From Figure 3.1, the fluids enters and exit at the same position ($X = 0$) for both flow arrangements A and B. Then the fluids exit temperature can be written as,

$$\theta_{ex} = \theta_m(X_{(j=1)} = 0)$$

Therefore the bayonet tube exit temperature from Equation 3.20 is given by,

$$\theta_{ex} = \theta_m(X_{(j=1)} = 0) = 1 - \int_{X=0}^L \theta_{\infty} dX \quad (3.21)$$

Where the subscript m is 1 for flow A and 2 for flow B.

Furthermore, the boundary conditions given by Equations 3.3 and 3.4 are also transformed into dimensionless form by using the dimensionless parameters stated earlier,

$$\text{at } X = 0 \quad \theta_z = 1 \quad (3.22)$$

$$\text{at } X = \frac{h_{01}p_{01}L}{mc_p} = \text{NTU}, \quad \theta_1 = \theta_2 \quad (3.23)$$

3.2 The effectiveness (ε): For the effectiveness of bayonet tube heat exchanger, due to the constant wall temperature of outer tube surface, the tube side fluid has maximum temperature difference then the shell side and from the definition of effectiveness,

$$\varepsilon = \frac{\dot{Q}}{\dot{Q}_{max}}$$

$$\varepsilon = \frac{h_{01}p_{01}}{C_{min}} \int_{x=0}^{x=L} \frac{(T_w - T_{\infty})}{(T_{in} - T_{\infty})} dx \quad (3.22)$$

Simplifying the above Equation 3.22 we obtained,

$$\varepsilon = \frac{h_{01}p_{01}}{C_{min}} \int_{x=0}^{x=L} \frac{-(T_{in} - T_w) \left[\frac{T_{\infty} - T_w}{T_{in} - T_w} \right]}{(T_{in} - T_w) \left[1 - \frac{T_{\infty} - T_w}{T_{in} - T_w} \right]} dx \quad (3.23)$$

Using definition of dimensionless shell side fluid temperature and Equation 3.17 for dimensionless flow length, Equation 3.23 is transformed and with further mathematical manipulation gives the effectiveness of the bayonet tube heat exchanger as,

$$\varepsilon = \int_{X=0}^{X=L} (1 - \theta_{\infty}) dX \quad (3.24)$$

CHAPTER 4 NUMERICAL TECHNIQUES

Introduction

4.1 Approximate Solution of Ordinary Differential Equations

The process of many physical systems is described by the ordinary differential equation, mostly transient systems. The solution of the equations are generated numerically or in some few cases are determined analytically (Carnahan et al., 1969). Consider a first order system of the form,

$$\frac{dy}{dx} = f(x, y) \quad (4.1)$$

Our target is to determine the solution $y(x)$ that satisfy Equation 4.1 and one boundary condition, such solution cannot be determined analytically alternatively, the intervals of independent variable x for which the solution is obtained $[a, b]$ is **divided into subintervals or steps by**

$$h = \frac{b - a}{n} \quad (4.2)$$

Where n refers to the number of steps and h is the numerical step size.

The true approximate solution of $y(x)$ is obtain at $n + 1$ for evenly spaced values of x (x_0, x_1, \dots, x_n) and the value of independent variable x at $n + 1$ is given by

$$x_{i+1} = x_i + ih \quad i = 0, 1, 2 \dots \dots n. \quad (4.3)$$

The solution of $y(x)$ for $n + 1$ discrete value of x is given in tabular form in Figure 4.1. Sampled values of one particular approximation can be obtained from the table of values (Carnahan et al., 1969).

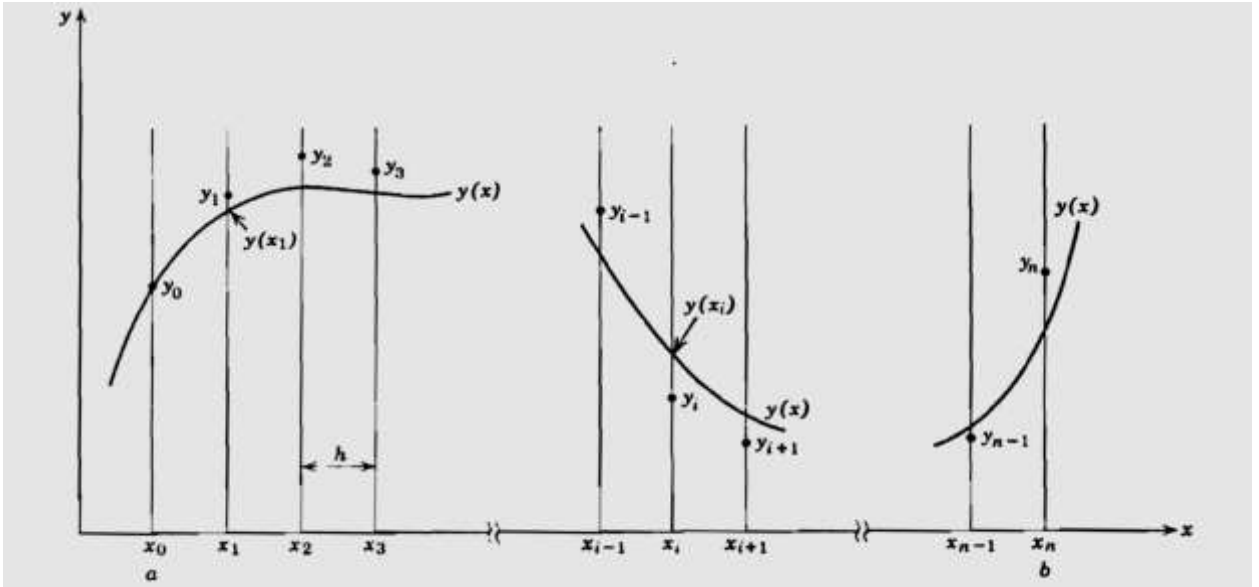


Figure 4.1: Numerical solution of first order ordinary differential equation

For the true solution $y(x)$ at specified base point be represented by $y(x_i)$ and the computed approximate solution $y(x)$ at that particular point by y_i such that

$$y_i = y(x_i) \quad (4.4)$$

The discretization error for that point is defined as difference between computed y_i and the true value $y(x_i)$ (Carnahan et al., 1969).

$$e_r = y_i - y(x_i) \quad (4.5)$$

The most common used numerical approach for the solution of first order ordinary differential equation with initial condition $y(x_0)$ are,

1. Direct or indirect use of Taylor's expansion of the solution function $y(x)$
2. The use of open or closed integration formulas.

4.1.1 Taylor's expansion approach

This method uses Taylor's expansion $y(x)$ about starting point x_0 , the numerical approximate solution of first order ordinary differential equation given by Equation 4.1 is

$$y(x_0 + h) = y(x_0) + hf(x_0, y(x_0)) + \frac{h^2}{2!} f'(x_0, y(x_0)) + \frac{h^3}{3!} f''(x_0, y(x_0)) + \dots \quad (4.6)$$

4.1.2 Runge-Kutta methods

The accuracy of Taylor's series approach is achieved using Runge-Kutta methods without the need of calculating higher derivatives (Chapra, 2012). The methods developed around 1900 by two German mathematicians C. Runge and M. W. Kutta. Among the several Runge-Kutta methods the fourth order Runge-Kutta is known for the precise solution of the ordinary differential equation. The fourth order Runge-Kutta for the solution of Equation 4.1 is given by,

$$y_{i+1} = y_i + \frac{1}{6}(k_1 + 2k_2 + 2k_3 + k_4)h \quad (4.7)$$

Where,

k_1, k_2, k_3 and k_4 are values of the approximate derivatives evaluated on the interval $x_i \leq x \leq x_{i+1}$.

$$k_1 = f(x_i, y_i) \quad (4.8)$$

$$k_2 = f\left(x_i + \frac{1}{2}h, y_i + \frac{1}{2}k_1h\right) \quad (4.10)$$

$$k_3 = f\left(x_i + \frac{1}{2}h, y_i + \frac{1}{2}k_2h\right) \quad (4.11)$$

$$k_4 = f(x_i + h, y_i + hk_3) \quad (4.12)$$

4.2 Numerical Integration

The approximation of the definite integral of a function using weighted sum method of function values at a particular point is term as numerical integration. Newton's cotes formulae are used for integration of simple interpolating polynomials with evenly spaced points. Among the formulae are trapezoidal and Simpson rule. The trapezoidal rule is based on values of the function at the end of the interval and the Simpson's rule credited to an England mathematician Thomas Simpson (1710 – 1761), in the method the two intervals and midpoint are connected by a parabola (Fausett, 1999).

Consider an interval of function $f(x)$ as $[a, b]$, using the point $x_i = a + ih$ $i = 1, 2, \dots, 2m$ the interval is divided in to $2m$ interval for $m \geq 2$ and the step size h is given as

$$h = \frac{b - a}{2m} \quad (4.8)$$

Generally, for an interval $[x_{2i-2}, x_{2i}]$ $i = 1, 2, \dots, m$, the Simpson's rule is stated as

$$\int_a^b f(x)dx = \frac{h}{3} [f(x_0) + 4f(x_1) + 2f(x_2) + 4f(x_3) + \dots + 2f(x_{2m-2}) + 4f(x_{2m-1}) + f(x_{2m})] \quad (4.9)$$

4.3 Numerical Model of Governing Equations

The steady state bayonet tubes temperature differential Equations 3.9 and 3.13 obtained are coupled first order ordinary differential equations, the approximate solution of these equations can be obtained numerically using the methods described in section 4.1 above together with two temperatures conditions at inlet given by Equation 3.22 and exit obtained using Equation 3.21 for specified value of shell side fluid temperature θ_∞ satisfying exchanger energy balance. The steps for numerical solution of temperature field are as follows

1. The bayonet tubes heat transfer length is discretized into n number of nodes from bayonet tube exchanger inlet $X_{(j=1)} = 0$ to the tubes sealed end $X_{(j=n)} = L$ with step size h as shown in Figure 3.1
2. The location of particular nodal point j , from the exchanger inlet is given by,

$$X_j = (j - 1)h = NTU_j \quad j = 1, 2, 3, \dots, n$$
3. The dimensionless temperatures of inner tube θ_2 and the annulus side θ_1 are function of four parameters of number of transfer unit (NTU), Hurd number (Hu), ratio of convective coefficients for outer tube (ξ) and flow arrangement.

$$\theta = f(NTU, Hu, \xi \text{ and flow arrangement}).$$

The temperatures distribution are obtained from selected values of Hu and ξ over the ranges $0.1 \leq Hu \leq 0.5$ and $0.6 \leq \xi \leq 0.9$ for both flow arrangement A and B satisfying exchanger balance.

4. The exchanger inlet temperature initial condition is taken for flow path A and B as described by Equation 3.22.
5. The exit temperature condition of bayonet tube at $X_{(j=1)} = 0$, i.e. θ_1 for flow arrangement A and θ_2 for flow arrangement B are determined from Equation 3.21 for specified value of shell temperature θ_∞ satisfying the exchanger energy balance.

6. The two dimensionless governing equations are integrated simultaneously using fourth order Runge-Kutta method given by Equation 4.7 with temperatures conditions described in steps 4 and 5 above.

The algorithm for flow arrangement A using above mentioned steps is as follows,

From steady state temperatures dimensionless governing equations

$$\frac{d\theta_1}{dX} = f_1(X, \theta_1, \theta_2) = \text{Hu}(\theta_1 - \theta_2) + \xi\theta_1$$

$$\frac{d\theta_2}{dX} = f_2(X, \theta_1, \theta_2) = \text{Hu}(\theta_1 - \theta_2)$$

The value of Hu and ξ are selected for step one above and the exit temperature of the exchanger $\theta_{ex} = \theta_1(X_{(j=1)} = 0)$ determined using step five above and also the inlet temperature condition at $X_{(j=1)} = 0$ given by $\theta_2(X_{(j=1)} = 0) = \theta_{in}$.

The solution domain is discretized such that

$$X_{j+1} = X_j + h,$$

Where h is step size,

Using fourth Runge-Kutta method with step size of 0.001, the solutions of temperature field at adjacent point $(X_{(j+1)})$ are determined by,

$$\theta_1(X_{(j+1)}) = \theta_1(X_j) + 1/6 (K_1\theta_1 + 2K_2\theta_1 + 2K_3\theta_1 + K_4\theta_1) \times h$$

$$\theta_2(X_{(j+1)}) = \theta_2(X_j) + 1/6 (K_1\theta_2 + 2K_2\theta_2 + 2K_3\theta_2 + K_4\theta_2) \times h$$

Where,

$K_1\theta, K_2\theta, K_3\theta$ and $K_4\theta$ are approximate derivatives values evaluated on $X_j \leq X \leq X_{j+1}$ interval, and they are defined as (Carnahan et. al, 1969).

$$K_1\theta_1 = hf_1(X_j, \theta_1, \theta_2)$$

$$K_1\theta_2 = hf_2(X_j, \theta_1, \theta_2)$$

$$K_2\theta_1 = hf_1(X_j + 0.5h, \theta_1(X_j) + 0.5K_1\theta_1h, \theta_2(X_j) + 0.5hK_1\theta_2)$$

$$K_2\theta_2 = hf_2(X_j + 0.5h, \theta_1(X_j) + 0.5hK_1\theta_1, \theta_2(X_j) + 0.5hK_1\theta_2)$$

$$K_3\theta_1 = hf_1(X_j + 0.5h, \theta_1(X_j) + 0.5hK_2\theta_1, \theta_2(X_j) + 0.5hK_2\theta_2)$$

$$K_3\theta_2 = hf_2(X_j + 0.5h, \theta_1(X_j) + 0.5hK_2\theta_1, \theta_2(X_j) + 0.5hK_2\theta_2)$$

$$K_4\theta_1 = hf_1(X_j + h, \theta_1(X_j) + hK_3\theta_1, \theta_2(X_j) + hK_3\theta_2)$$

$$K_4\theta_2 = hf_2(X_j + h, \theta_1(X_j) + hK_3\theta_1, \theta_2(X_j) + hK_3\theta_2)$$

The determination of temperatures θ_1 and θ_2 continuous up to the bayonet tube sealed end $X_{(j=n)} = L$. The computation of temperatures field is terminated with graphical representation of the two temperatures distribution satisfying the energy balance.

For the case of reverse flow B shown in Figure 3.1, by the white arrow, the algorithm differs slightly from flow A. For flow arrangement A the exit temperature obtained from Equation 3.21 is taken to be $(\theta_1)_{j=1}$ and for the reverse flow B as $\theta_{ex} = \theta_2(X_{(j=1)} = 0)$, beside this, all other steps are the same with flow arrangement A algorithm.

Moreover, the algorithm for determination of exit temperatures $\theta_{ex} = \theta_m(X_{(j=1)} = 0)$ using Simpson's one third rule, for step three above is given below,

$$\begin{aligned} \theta_m(X_{(j=1)} = 0) &= 1 - \int_{X=0}^{X=L} \theta_{\infty} dX \\ &= 1 - \left[\frac{h}{3} (\theta_{\infty}(X_{j=1}) + 4\theta_{\infty}(X_{j+1}) + 2\theta_{\infty}(X_{j+2}) + \theta_{\infty}(X_{j+3}) + \dots + 4\theta_{\infty}(X_{j=L-1}) \right. \\ &\quad \left. + \theta_{\infty}(X_{j=L})) \right] \end{aligned}$$

The specified value of shell side temperature θ_{∞} satisfying exchanger energy balance is assumed throughout the analysis.

CHAPTER 5

RESULTS AND DISCUSSION

5.1 Results and Discussion

Using an energy balance on control volume of bayonet tube heat exchanger, the steady state temperature differential equations, and the related boundary conditions are obtained for two flow arrangements A and B and transformed into the dimensionless form using dimensionless parameters of temperatures and flow length.

From the dimensionless governing equations obtained, the temperatures of inner tube θ_2 and that of annulus side θ_1 of a bayonet tube heat exchanger are determined to be function of four parameters of number of transfer unit (NTU), Hurd number (Hu), ratio of convective coefficient of the outer tube surfaces (ξ) and flow arrangements presented as,

$$\theta = \phi(\text{NTU}_x, \text{Hu}, \xi \text{ and flow arrangement})$$

Graphical representation of tube temperature distributions is obtained for specified design parameters of Hu and ξ from the ranges stated earlier for both flow arrangement A and B. Consider a typical temperature distribution of flow arrangement A with $\text{Hu} = 0.5$ and $\xi = 0.6$ presented in Figure 5.1, the large value of Hu (i.e. $\text{Hu} = 0.5$) indicates low annulus number of transfer unit (NTU) and it was observed that inner tube fluid has high temperature drop which decreases as Hu is decrease. For both flow arrangements A and B the value of NTU_x satisfying the exchanger energy balance increase from $\text{Hu} = 0.5$ to $\text{Hu} = 0.1$ as shown by Figures 5.3 and 5.4 for reverse flow B and also Figures 5.1 and 5.2 for flow A. In the reverse flow B the tubes fluid temperatures has minimum value at tube tip $x = L$ and increases toward the bayonet tube exit due to the energy gained from the annulus by the inner tube fluid. However, the low values of Hu (i.e. $\text{Hu} = 0.1$) shown in Figures 5.2 and 5.4 which corresponds to case with high thermal conductance in annular side, the heat transfer between annulus and the inner tube was negligibly small as a result the bayonet tube behaves like a single tube a heat exchanger.

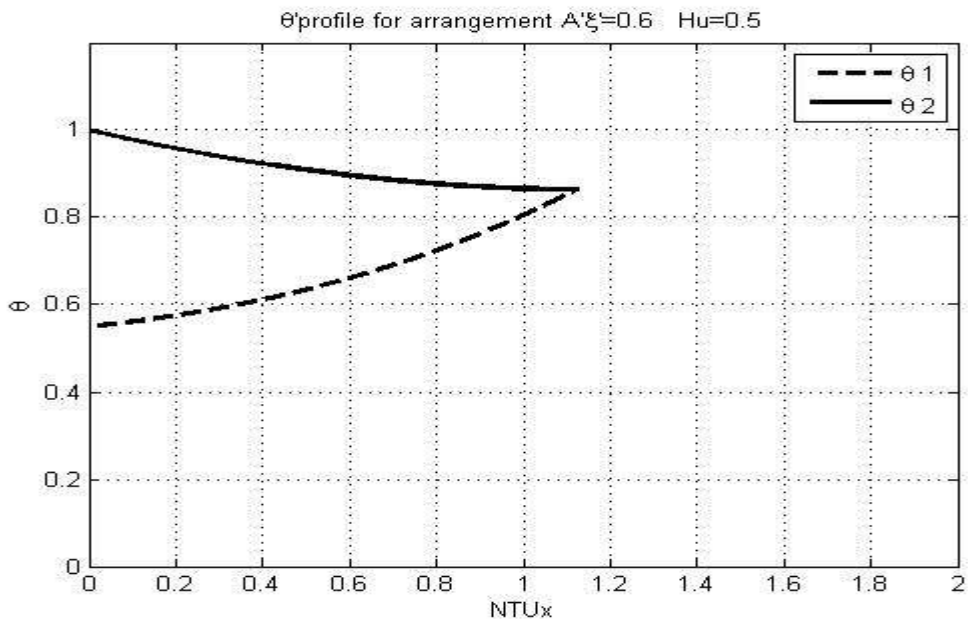


Figure 5.1: Temperature distribution for flow arrangement A $Hu=0.5$ and $\xi = 0.6$

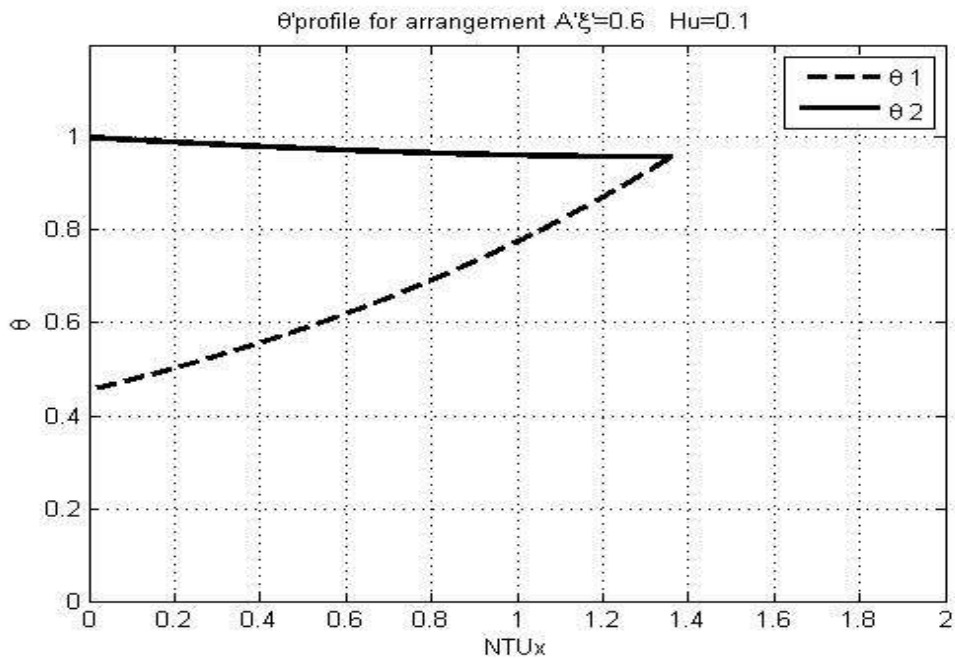


Figure 5.2: Temperature distribution for flow arrangement A $Hu=0.1$ and $\xi = 0.6$.

The convective heat transfer coefficient (h) is a proportionality constant that relates the heat flux and heat transfer driving force (fluids temperature difference). Heat transfer increases with increase in h . At a particular fluids temperatures the ratio of convective heat transfer coefficient of the outer tube surfaces ξ plays an important role in accessing heat transfer

from outer tube fluid to shell side of a bayonet tube heat exchanger. From Figure 5.2 and 5.5 at low Hu for flow arrangement A it was observed that ξ has less effect on temperature distribution, and due to the high temperature fluid in the annulus, its independent of Hu values in reverse flow B. the overall exchanger energy balance is attained at small value of NTU_x at lower a value of ξ . For all values of Hu in both flow A and B, the heat transfer from tubes to shell side is enhanced at $\xi = 0.9$ with lower exit temperature.

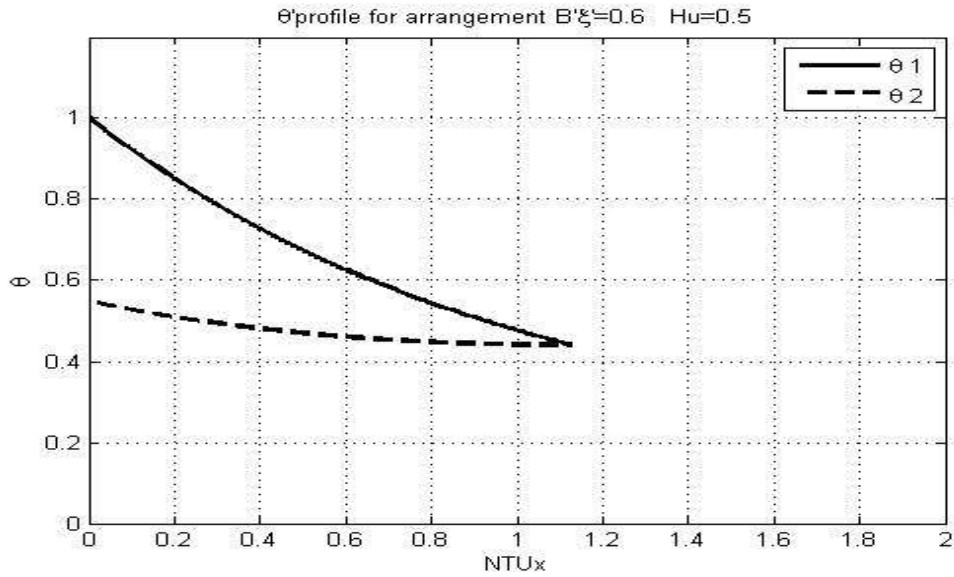


Figure 5.3: Temperature distribution for flow arrangement B $Hu=0.5$ and $\xi = 0.6$

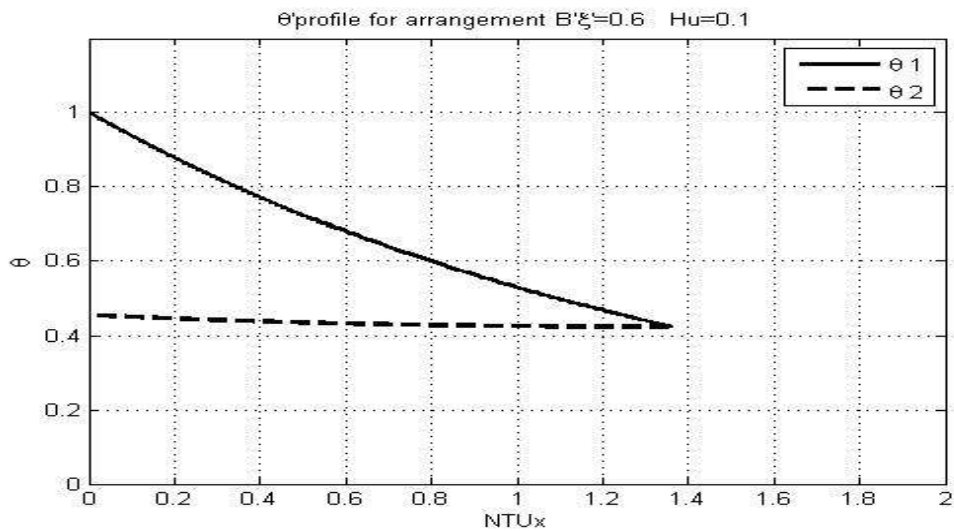


Figure 5.4 Temperature distribution for flow arrangement B $Hu=0.1$ and $\xi = 0.6$.

From the temperatures distribution obtained at various values of Hu and ξ , it's clearly indicated that the reversing of flow arrangement has significant effect on thermal design of

bayonet tube heat exchanger. Considering the case of flow arrangement A in which a fluid at high temperature enters through the inner tube, it is evident from Figures 5.1 and 5.2 that large temperature difference is attained between the tube tips and shell side fluid more especially at low Hu and less heat is transferred to the shell side. In reverse flow B Figures 5.2 and 5.3, the difference is very small particularly at large value of Hu resulting to high rates of heat transfer.

The essential factor to be considered in accessing thermal performance of heat exchanger is the effectiveness (ε) of the exchanger which is the measure of amount of heat transferred within infinite area. In the present analysis the effectiveness of bayonet heat exchanger is determined to be dependent on shell side fluid temperature θ_∞ and NTU_x as given by Equation 3.24. For particular value of NTU_x the ε increases with increase in rate of heat transfer to shell side. The dependence of the rate of heat transfer to shell side fluid temperature on the value of Hu and ξ relates the effectiveness to Hu and ξ . From Figures 5.2 and 5.4, at low value of a Hu , the reverse flow with high temperature fluid in the annulus is determined to have higher effectiveness. The tip temperature at $x = L$ has great significant in controlling tube side fluid temperatures, Table 6.1 present the values of tip temperatures at various values of Hu and ξ satisfying exchanger energy balance for two possible flow arrangements.

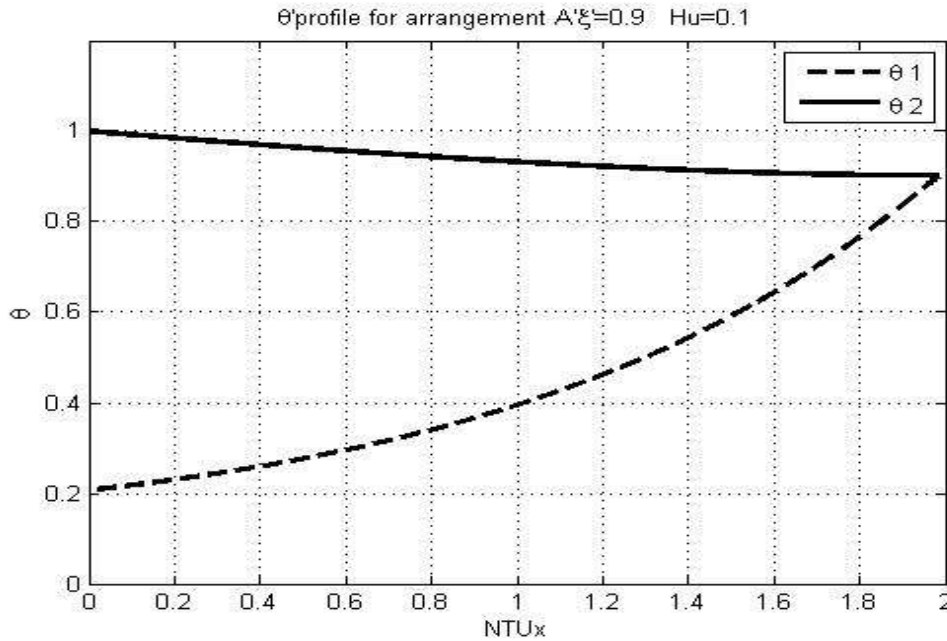


Figure 5.5: Temperature distribution for flow arrangement A $Hu=0.1$ and $\xi = 0.9$

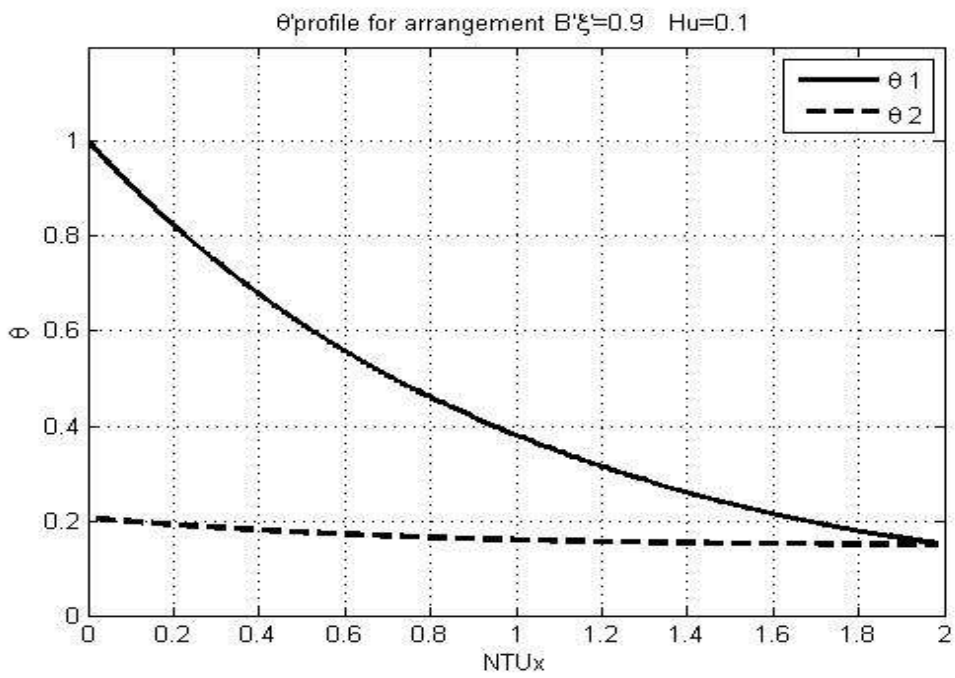


Figure 5.6: Temperature distribution for flow arrangement B $Hu=0.1$ And $\xi = 0.9$

Table 6.1: Values of tube tip temperature for flow arrangement A and B

Flow arrangement A				Flow arrangement B			
Hu	ξ	θ_1	θ_2	Hu	ξ	θ_1	θ_2
0.5	0.6	0.8646	0.8639	0.5	0.6	0.4401	0.4405
0.5	0.7	0.8162	0.8160	0.5	0.7	0.3078	0.3070
0.5	0.8	0.7473	0.7466	0.5	0.8	0.2229	0.2231
0.5	0.9	0.7031	0.7035	0.5	0.9	0.1613	0.1629
0.4	0.6	0.8811	0.8810	0.4	0.6	0.4363	0.4363
0.4	0.7	0.8240	0.8235	0.4	0.7	0.3069	0.3071
0.4	0.8	0.7757	0.7761	0.4	0.8	0.2203	0.2202
0.4	0.9	0.7358	0.7378	0.4	0.9	0.1613	0.1619
0.3	0.6	0.9022	0.9017	0.3	0.6	0.4336	0.4342
0.3	0.7	0.8534	0.8529	0.3	0.7	0.3033	0.3037
0.3	0.8	0.8132	0.8126	0.3	0.8	0.2168	0.2162
0.3	0.9	0.7811	0.7804	0.3	0.9	0.1591	0.1599
0.2	0.6	0.9270	0.9268	0.2	0.6	0.4296	0.4298
0.2	0.7	0.8887	0.8890	0.2	0.7	0.2997	0.3001
0.2	0.8	0.8602	0.8593	0.2	0.8	0.2134	0.2133
0.2	0.9	0.8350	0.8328	0.2	0.9	0.1556	0.1559
0.1	0.6	0.9580	0.9583	0.1	0.6	0.4238	0.4234
0.1	0.7	0.9350	0.9359	0.1	0.7	0.2938	0.2938
0.1	0.8	0.9167	0.9172	0.1	0.8	0.2090	0.2088
0.1	0.9	0.9003	0.9010	0.1	0.9	0.1510	0.1503

CHAPTER 6 CONCLUSION

6.1 Conclusion

The thermal design method of a bayonet tube heat exchanger with constant outer tube surface wall temperature is presented numerically. The exchanger is considered to have two flow arrangements as shown in figure 3.1. The tubes temperature differential equations and the related boundary conditions obtained from energy balance on the bayonet tube control volume are transformed into dimensionless form. The dimensionless temperature differential equations are presented as a function of Hurd number (Hu), the ratio of the convective coefficient (ξ), number of transfer unit (NTU) and flow arrangements.

The governing Equations 3.9 and 3.12 are solved numerically in the ranges of $0.1 \leq Hu \leq 0.5$ and $0.6 \leq \xi \leq 0.9$ for both flow arrangements using the inlet temperature condition given by Equation 3.22 and the exit temperature specified using Equation 3.21, the approximate solution of tube temperature is presented graphically for a particular value of Hu and ξ satisfying the exchanger energy balance. The effectiveness of the exchanger is determined as a function of shell side fluid temperature as illustrated by Equation 3.24.

From the temperatures distribution obtained, for a case with high thermal conductance in annulus side (at low Hu) less heat is exchanged between the tubes and the energy balanced is attained at large value of NTU_x , under the same condition the ξ has less effect on temperatures distribution for flow arrangement A. in reverse flow arrangement, the minimum temperature occur at tube tip result with higher heat transfer rates.

REFERENCES

- Cesar, G. (2013). Characterization of heat transfer and evaporative cooling of heat exchangers for sorption-based solar cooling application. *Master Thesis, Fraunhofer ISE*, Breisgau, Germany.
- Steven, C. (2012). *Applied Numerical Method for Scientist and Engineers with Matlab*. New York, McGraw-Hill.
- Frank, K., Raj M. M., and Mark, S. B. (2011). *Principles of Heat Transfer*. Stamford, Cengage.
- Khan, W. A., Culham, J. R., and Yovanovich M. M. (2006). Convection heat transfer from tube banks in cross flow, an analytical approach. *International Journal of Heat and Mass transfer*, 49, 4831- 4838.
- Ramesh, K. S., and Dusan, P. S. (2003). *Fundamentals of Heat Exchanger Design*. New Jersey, Wiley.
- Suli, E., and Mayers, D. (2003). *An Introduction to Numerical Analysis*. Cambridge, Cambridge University Press.
- Sadik, K., and Hongtan, L. (2002). *Heat Exchangers Selection, Rating, and Thermal Design*. New York, CRC Press.
- Theodore, L. B., Adrienne, S. L., Frank P. I., and David, P. D. (2002). *Introduction to Heat Transfer*. New York, Wiley.
- O'Doherty, T., Jolly, A. J., Bates, and C. J. (2001) Optimization of heat transfer enhancement devices in bayonet tube heat exchanger. *Journal of Applied Thermal Engineering* 21, 19-36.
- O'Doherty, T., Jolly, A. J., Bates, and C. J. (2001) Analysis of a bayonet tube heat exchanger. *Journal of Applied Thermal Engineering* 21, 1-18.
- Vedat, S. A., Ahmet, S., and Shu-Hsin, K. (2000). *Introduction to Heat Transfer*. Upper Saddle River, Prentice Hall.
- Kayansayan, N. (1996). The thermal design method of bayonet tube evaporators and condensers. *International Journal of Refrigeration*, 19 (3), 197- 207.

- Minhas, H., Lock, S. H., and Maolin, Wu. (1995). Flow characteristic of an air filled bayonet tube under the laminar condition. *International Journal of Heat and Fluid Flow*, 16 (3), 186-193.
- Harpal, S. M. (1993). A numerical analysis of laminar frictional characteristics of bayonet tube. *Master thesis, Mechanical Engineering Department University of Alberta, Alberta, Canada.*
- Kays, W., and London, A. (1984). *Compact Heat Exchangers* New York, McGraw-Hill.
- London, A. L., and Seban, R. A. (1980). A generalization of the method of heat exchanger analysis. *International Journal of Heat and Mass Transfer*, 28(2), 5-16.
- Carnahan, B., Luther, H. A., and Wilkes, J. O. (1969). *Applied numerical method*. New York, Wiley.
- Hurd, N. L. (1946). The mean temperature difference in field or bayonet tube heat exchanger. *Journal of Industrial and Chemical Engineering*, 38(12), 1266-1271.

APPENDICES

APPENDIX 1

TEMPERATURE DISTRIBUTION FOR FLOW ARRANGEMENT A

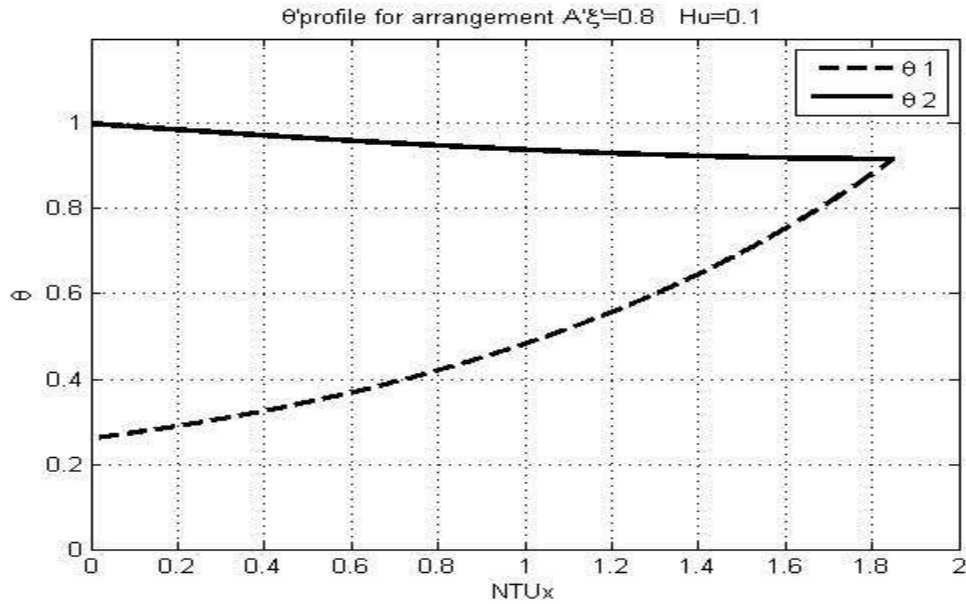


Figure 1.1: Temperatures distribution for flow arrangement A $\xi = 0.8$ and $Hu = 0.1$

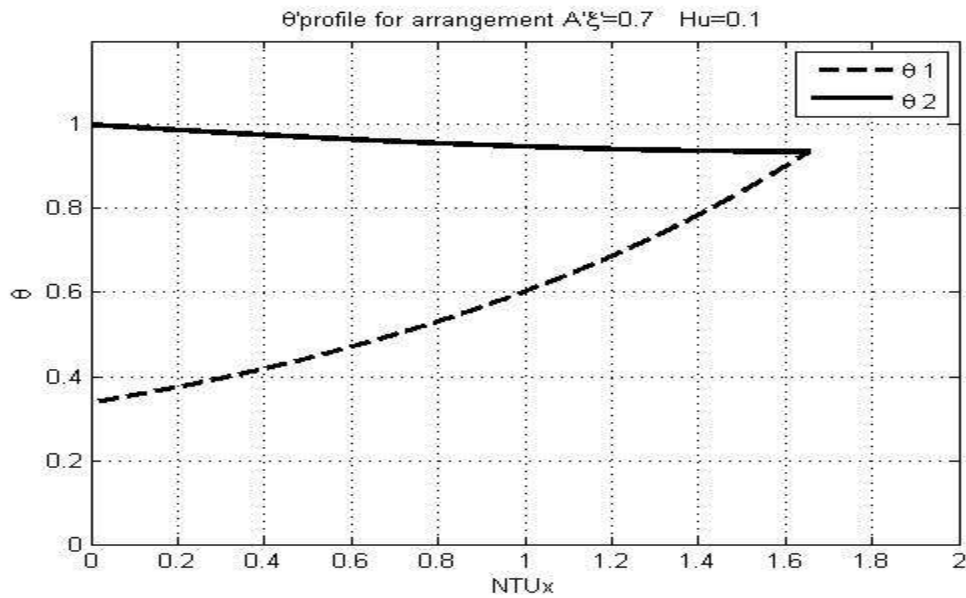


Figure 1.2: Temperatures distribution for flow arrangement A $\xi = 0.7$ and $Hu = 0.1$

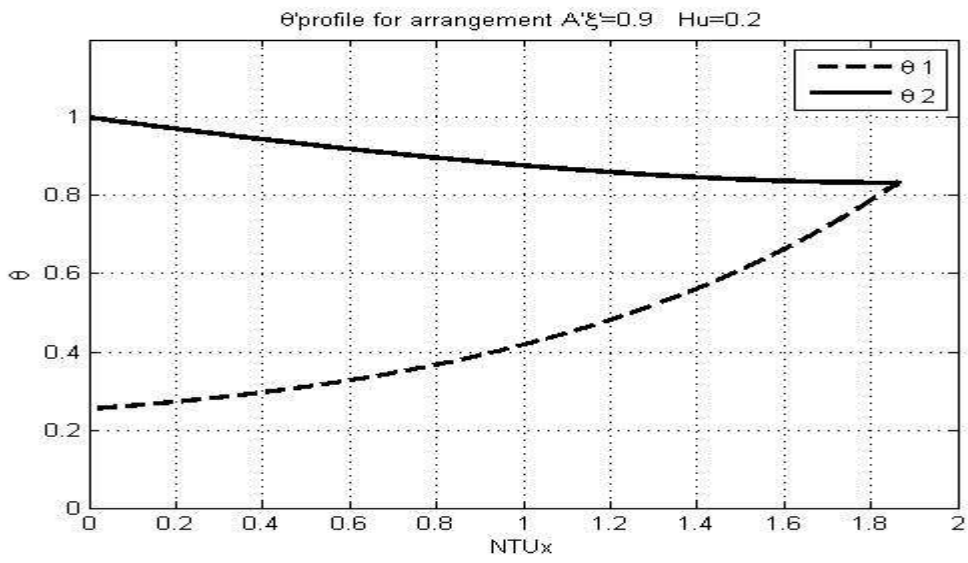


Figure 1.3: Temperatures distribution for flow arrangement A $\xi = 0.9$ and $Hu = 0.2$

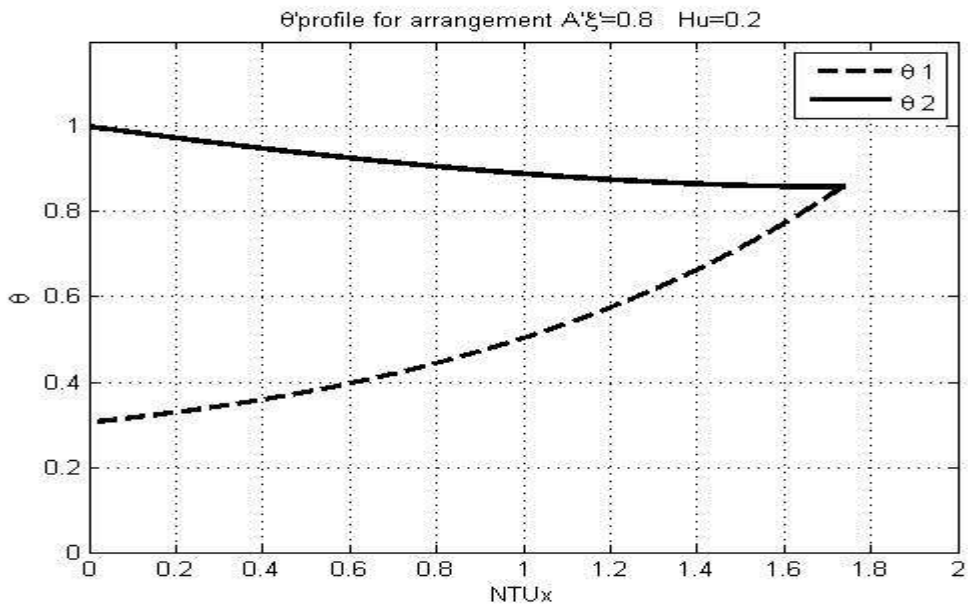


Figure 1.4: Temperatures distribution for flow arrangement A $\xi = 0.8$ and $Hu = 0.2$

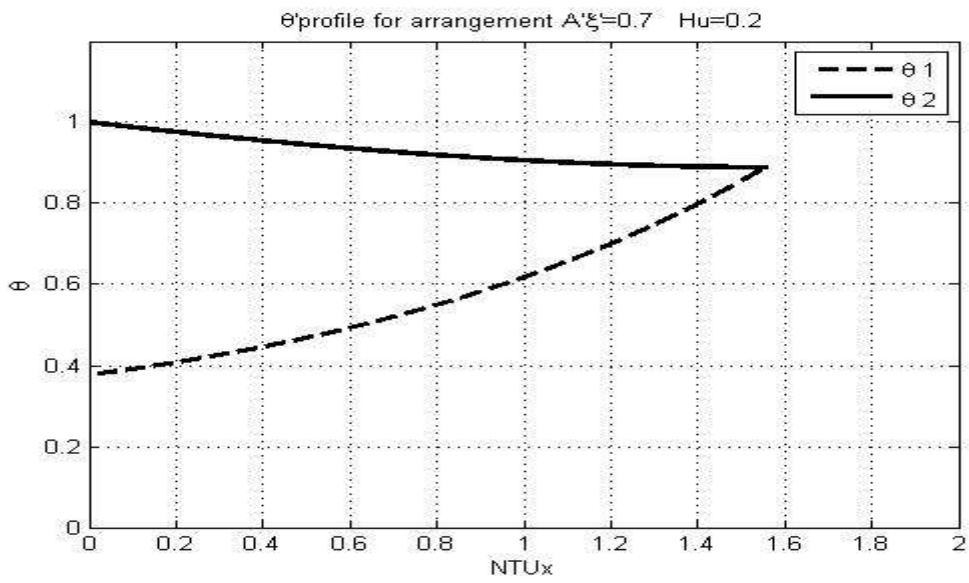


Figure 1.5: Temperatures distribution for flow arrangement A $\xi = 0.7$ and $Hu = 0.2$

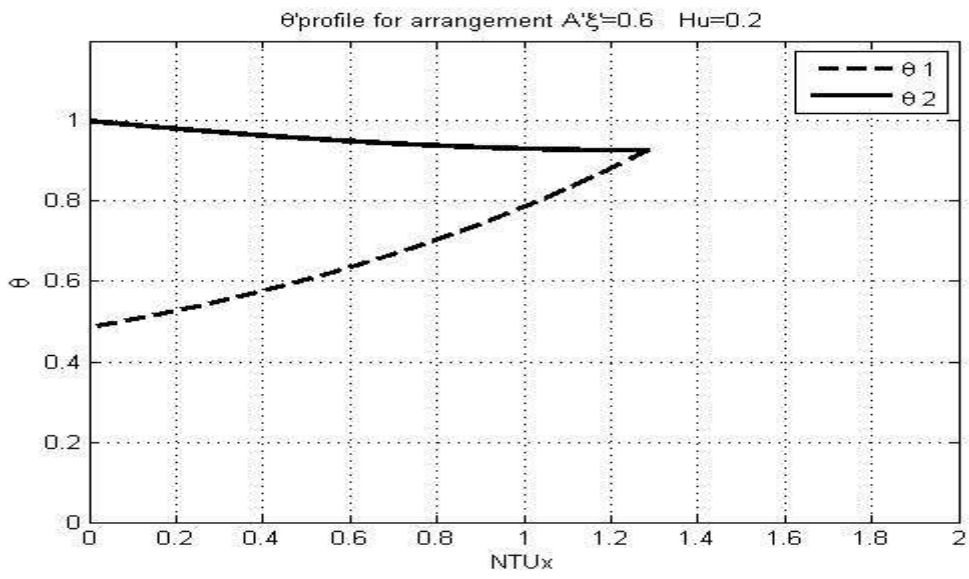


Figure 1.6: Temperatures distribution for flow arrangement A $\xi = 0.6$ and $Hu = 0.2$

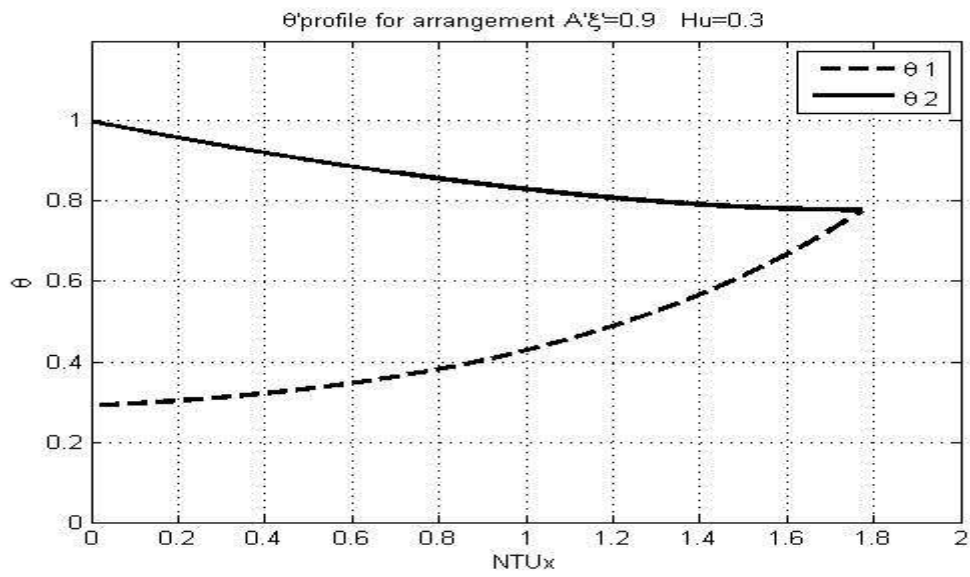


Figure 1.7: Temperatures distribution for flow arrangement A $\xi = 0.9$ and $Hu = 0.3$

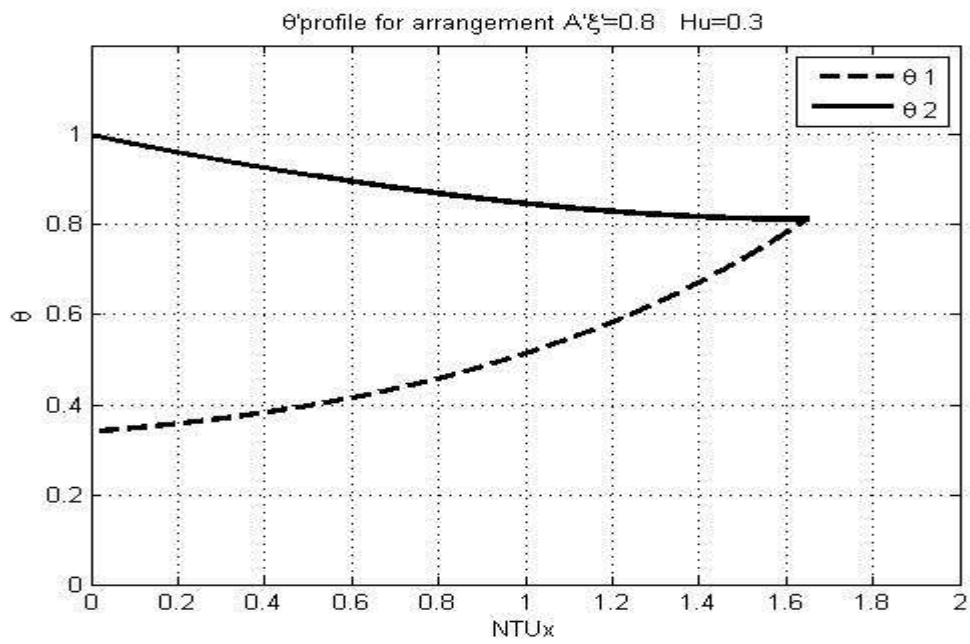


Figure 1.8: Temperatures distribution for flow arrangement A $\xi = 0.8$ and $Hu = 0.3$

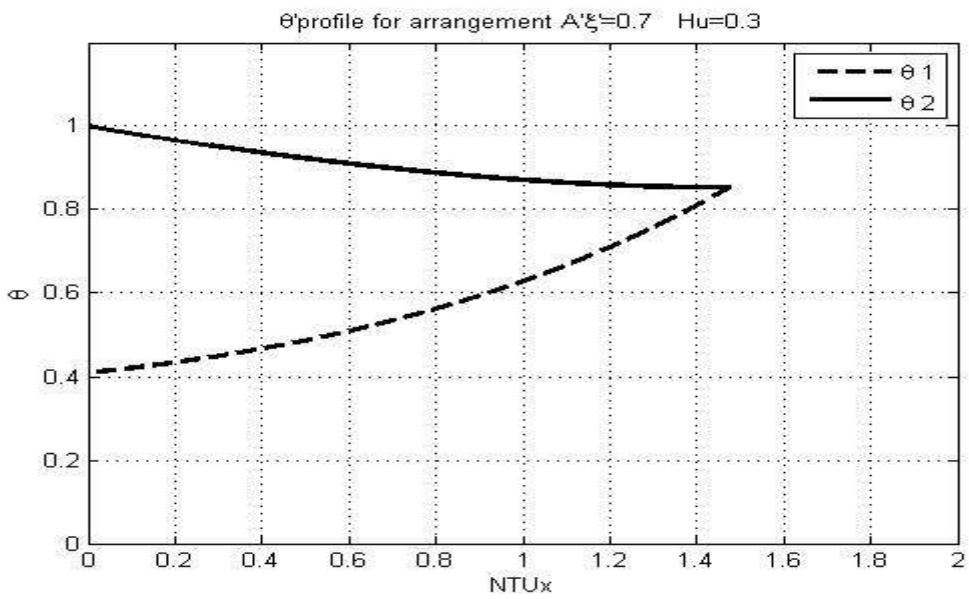


Figure 1.9: Temperatures distribution for flow arrangement A $\xi = 0.7$ and $Hu = 0.3$

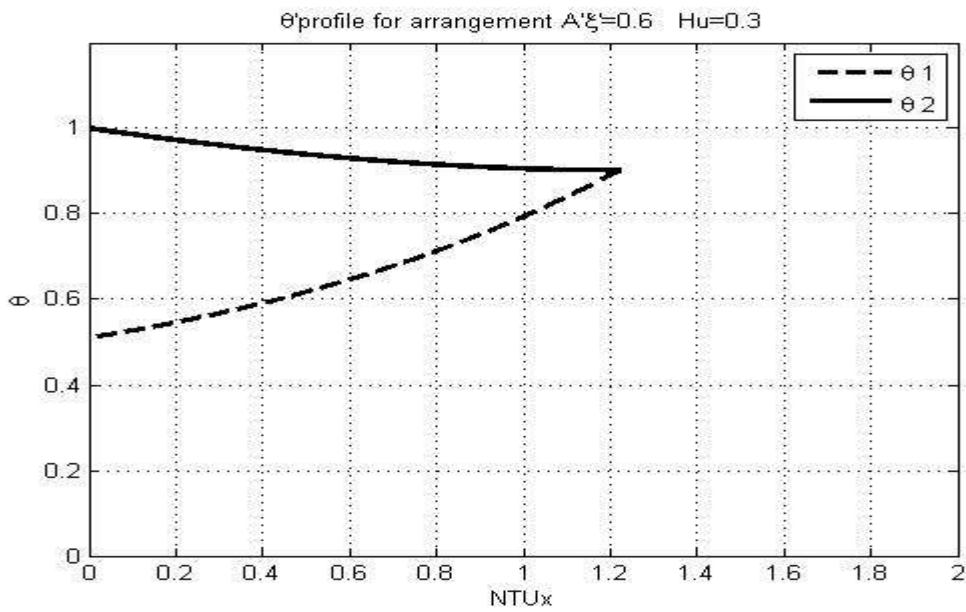


Figure 1.10: Temperatures distribution for flow arrangement A $\xi = 0.6$ and $Hu = 0.3$

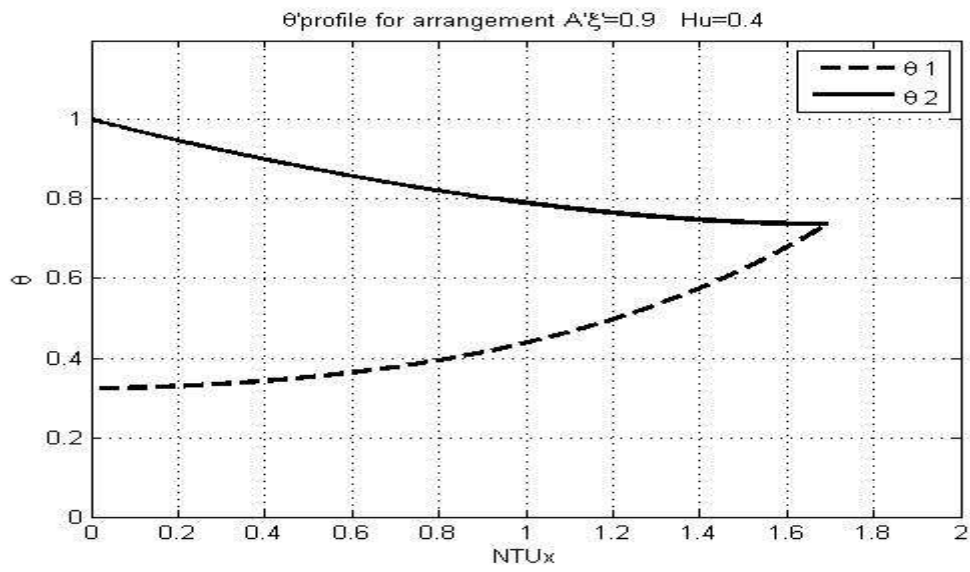


Figure 1.11: Temperatures distribution for flow arrangement A $\xi = 0.9$ and $Hu = 0.4$

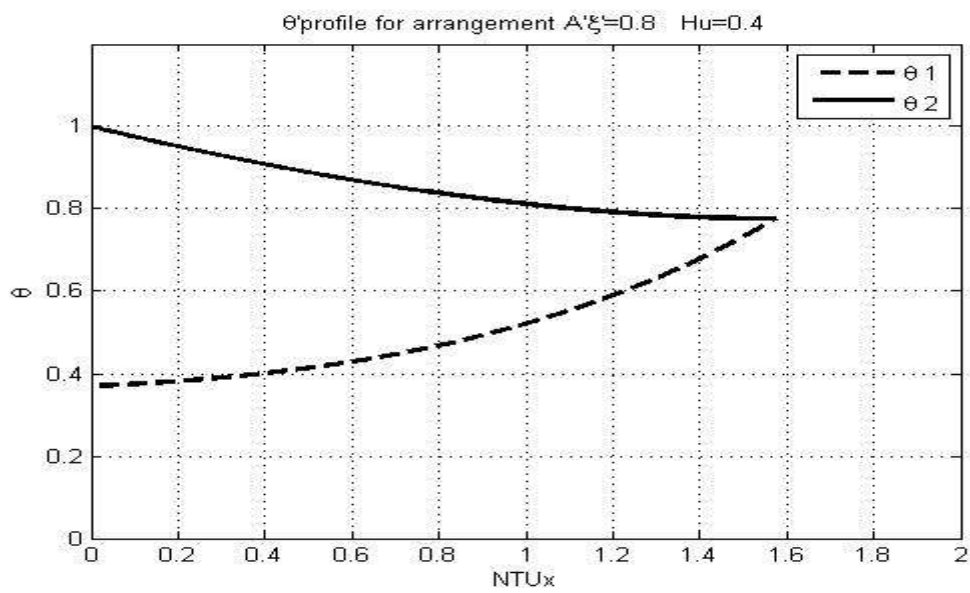


Figure 1.12: Temperatures distribution for flow arrangement A $\xi = 0.8$ and $Hu = 0.4$

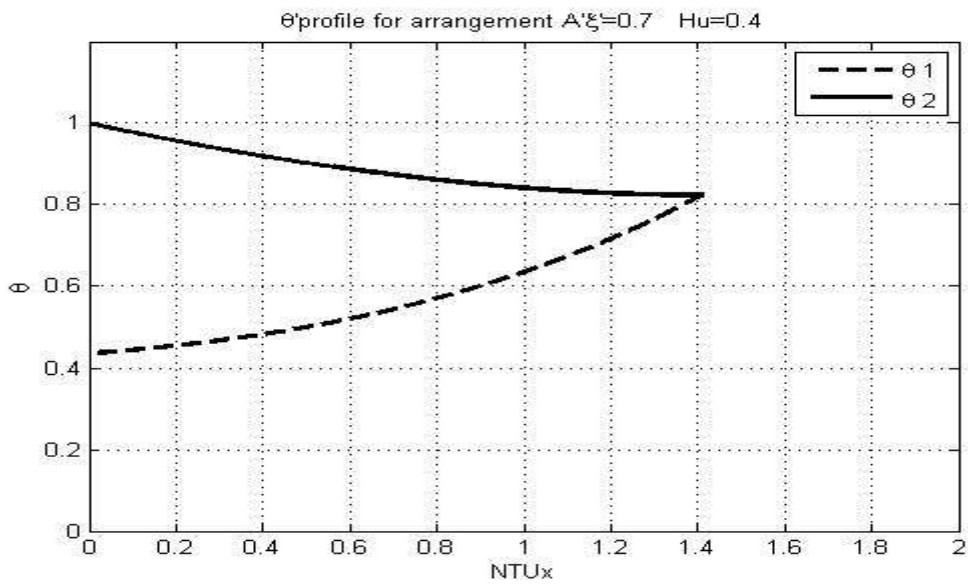


Figure 1.13: Temperatures distribution for flow arrangement A $\xi = 0.7$ and $Hu = 0.4$

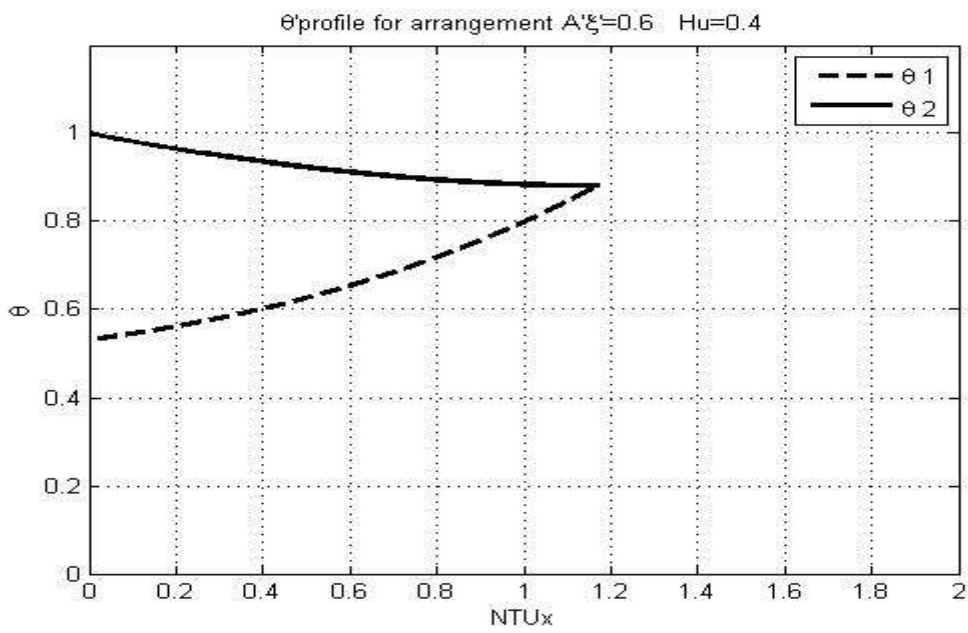


Figure 1.14: Temperatures distribution for flow arrangement A $\xi = 0.6$ and $Hu = 0.4$

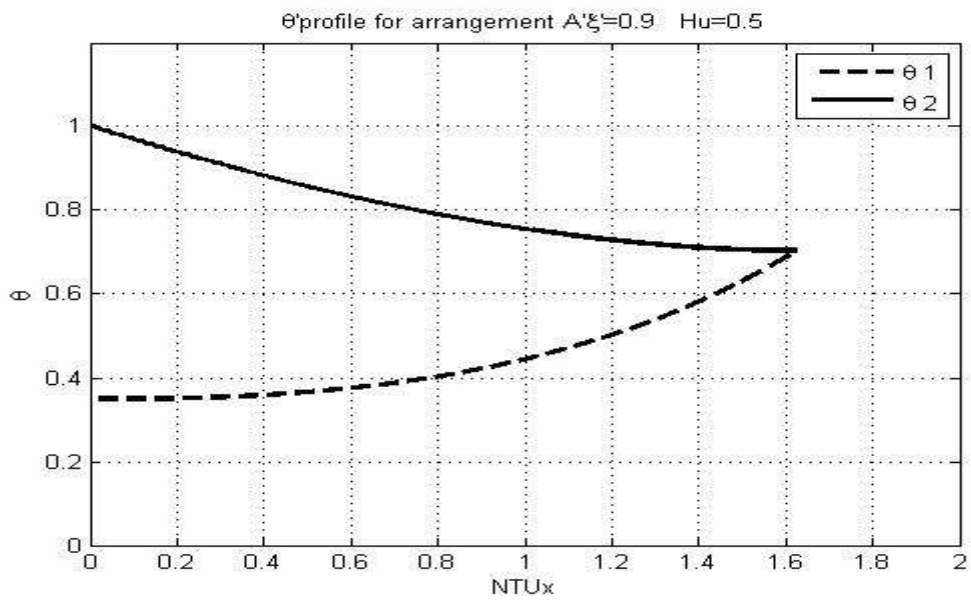


Figure 1.15: Temperatures distribution for flow arrangement A $\xi = 0.9$ and $Hu = 0.5$

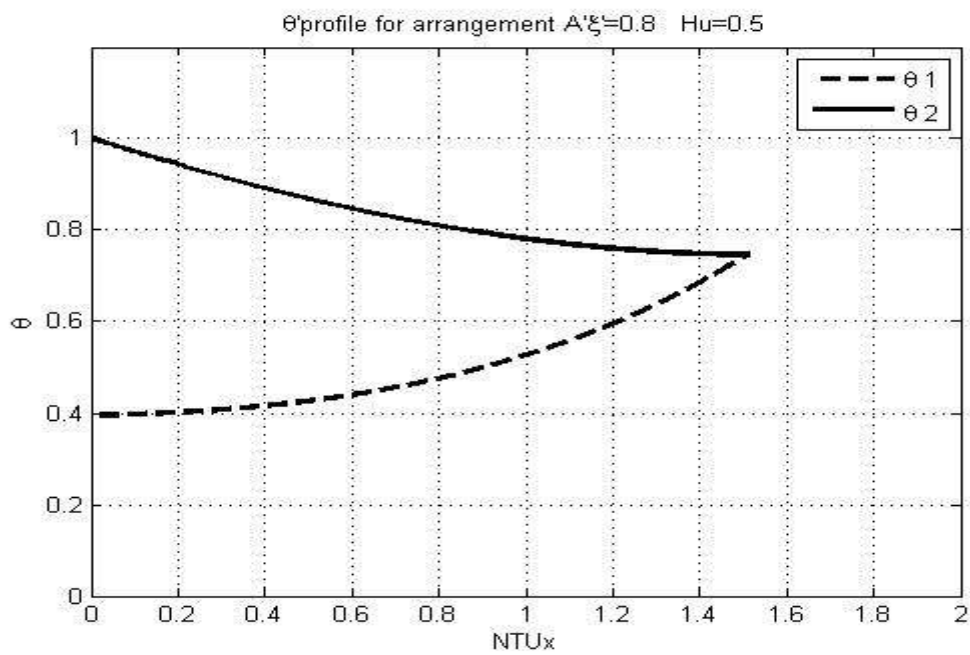


Figure 1.16: Temperatures distribution for flow arrangement A $\xi = 0.8$ and $Hu = 0.5$

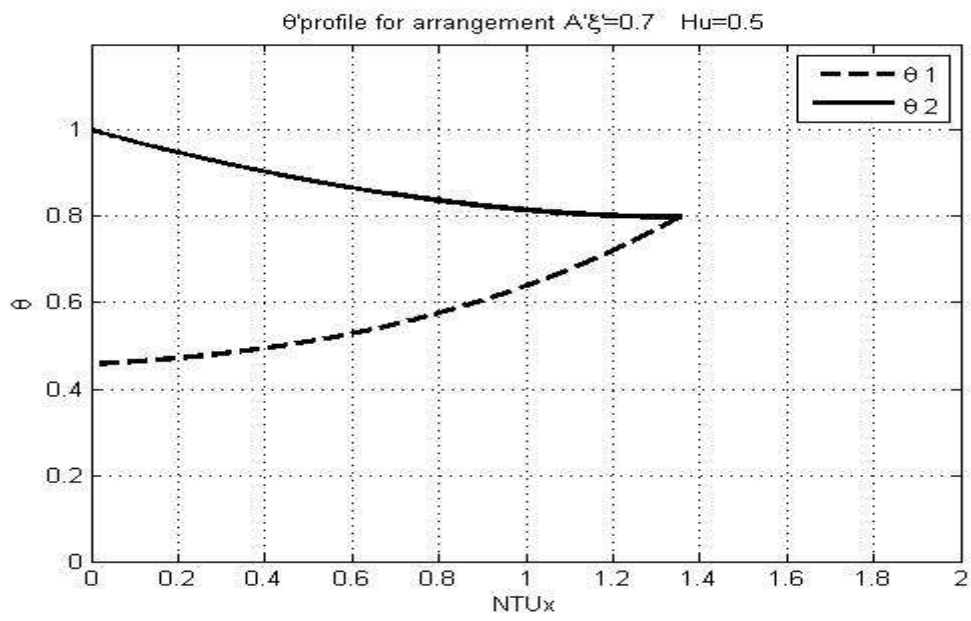


Figure 1.17: Temperatures distribution for flow arrangement A $\xi = 0.7$ and $Hu = 0.5$

APPENDIX 2

TEMPERATURE DISTRIBUTION FOR FLOW ARRANGEMENT B

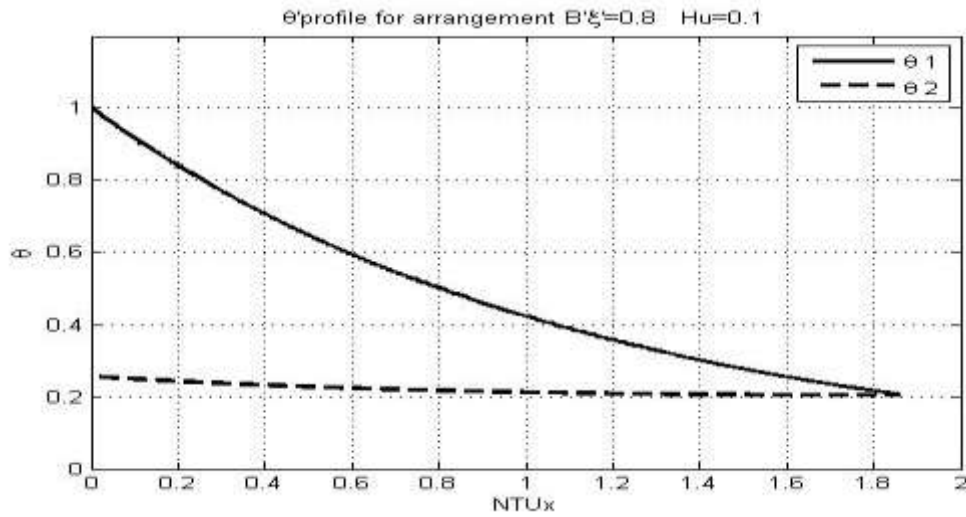


Figure 2.1: Temperatures distribution for flow arrangement B. $\xi = 0.8$ and $Hu = 0.1$

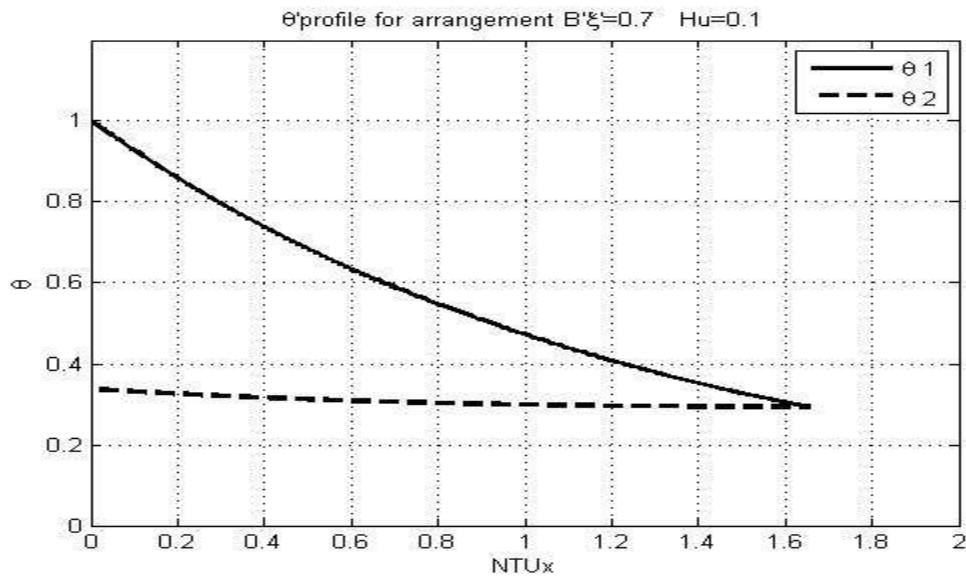


Figure 2.2: Temperatures distribution for flow arrangement B. $\xi = 0.7$ and $Hu = 0.1$

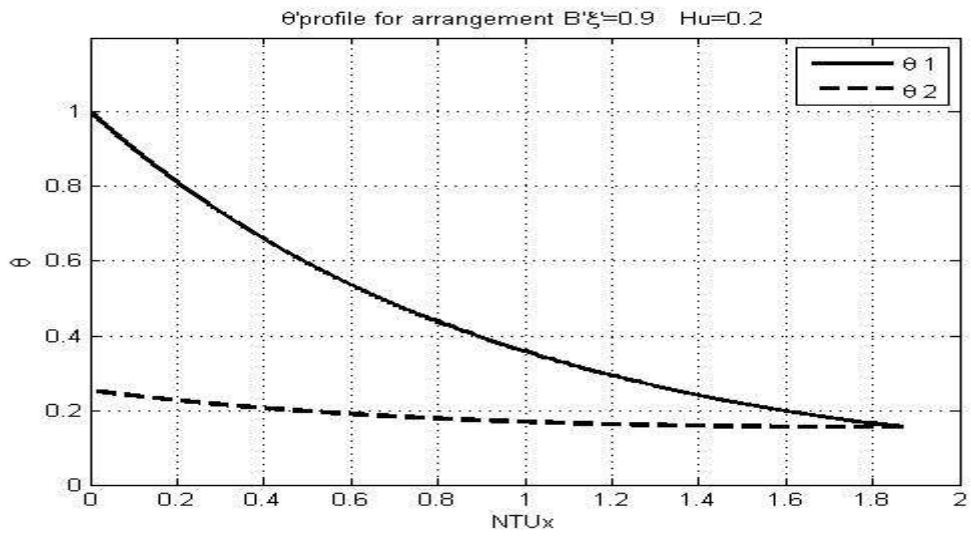


Figure 2.3: Temperatures distribution for flow arrangement B. $\xi = 0.9$ and $Hu = 0.2$

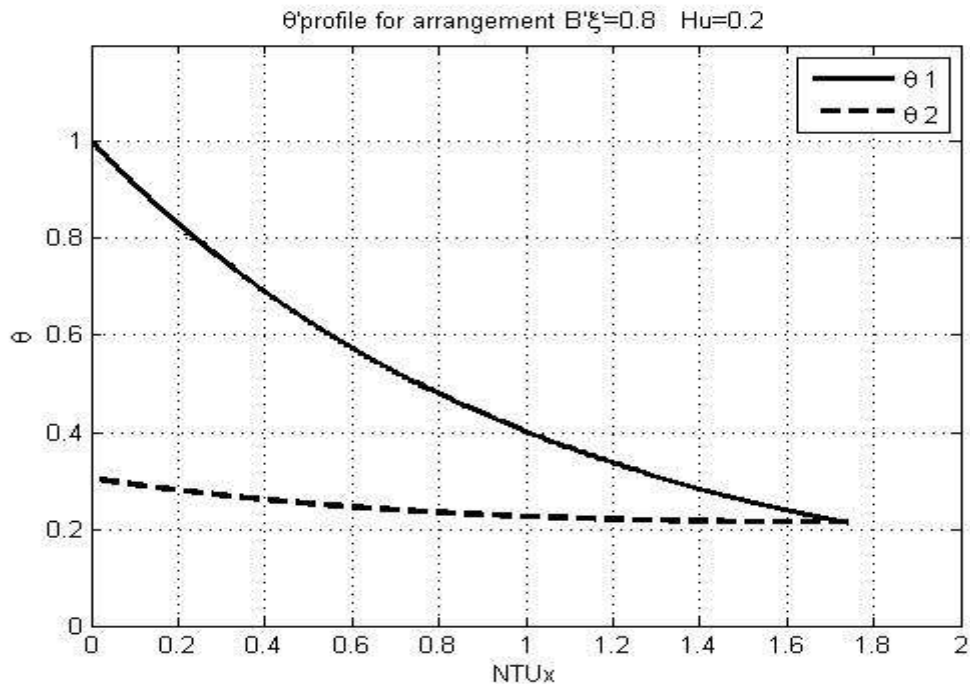


Figure 2.4: Temperatures distribution for flow arrangement B. $\xi = 0.8$ and $Hu = 0.2$

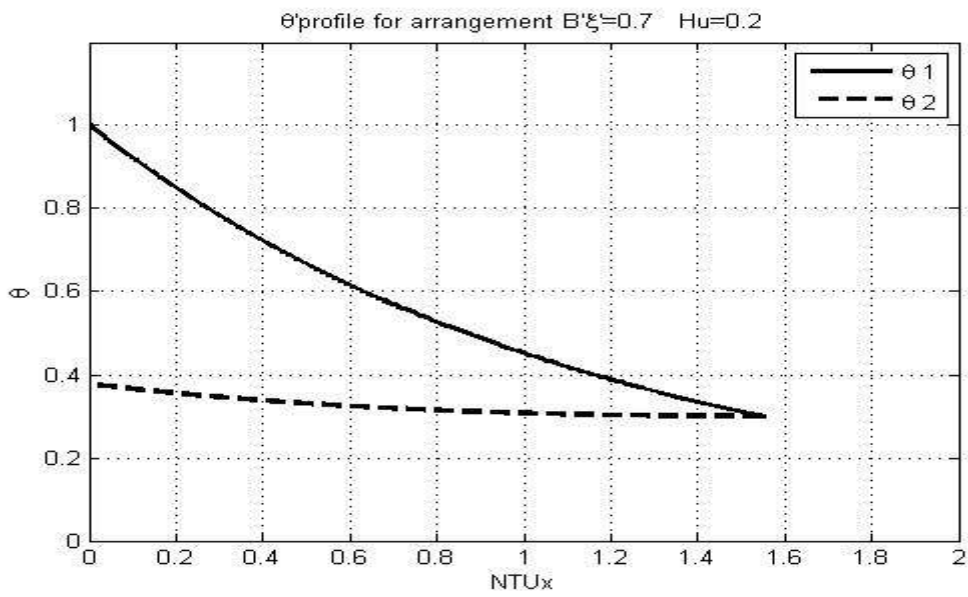


Figure 2.5: Temperatures distribution for flow arrangement B. $\xi = 0.7$ and $Hu = 0.2$

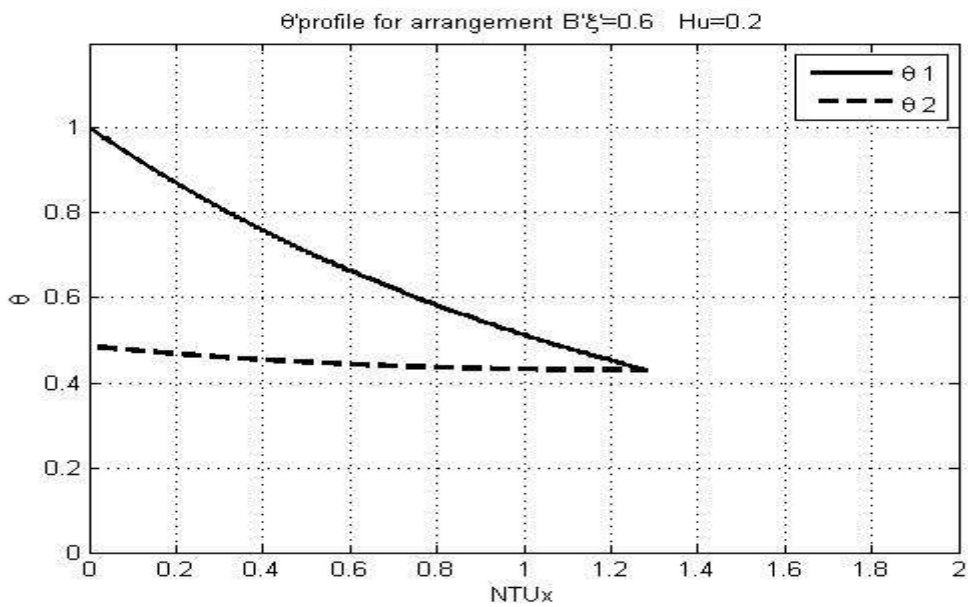


Figure 2.6: Temperatures distribution for flow arrangement B $\xi = 0.6$ and $Hu = 0.2$

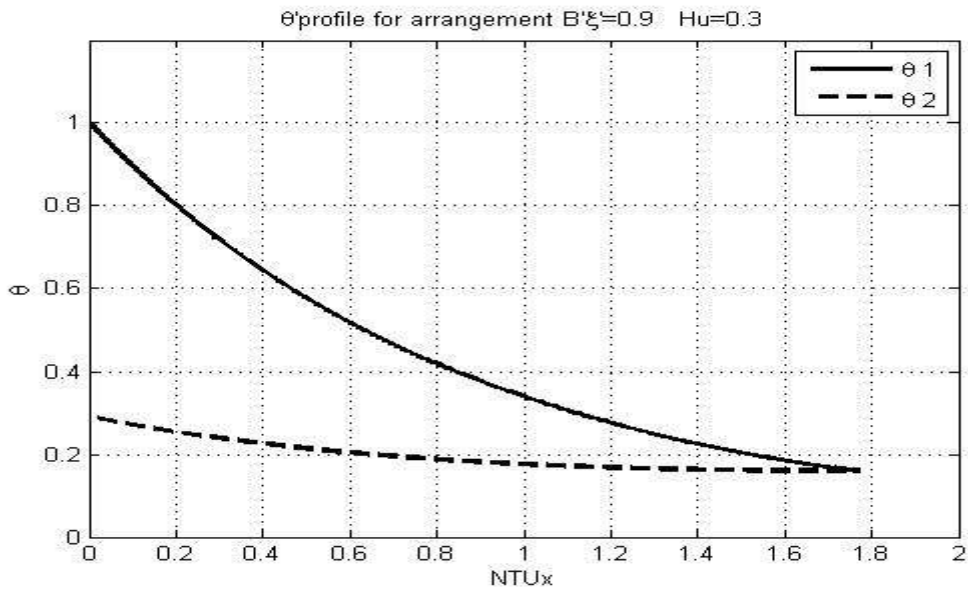


Figure 2.7: Temperatures distribution for flow arrangement B. $\xi = 0.9$ and $Hu = 0.3$

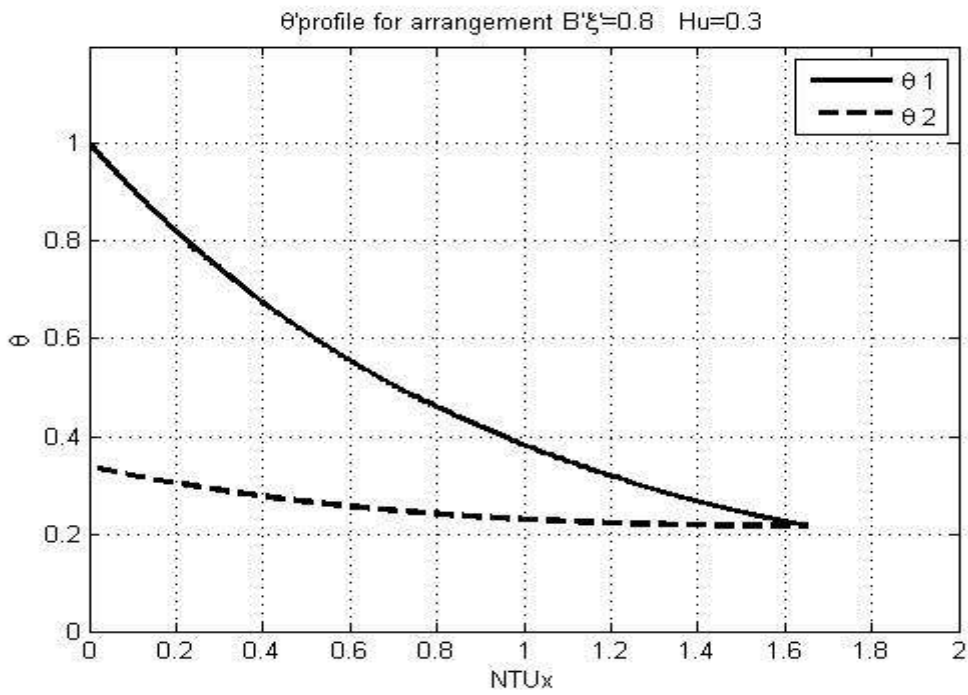


Figure 2.8: Temperatures distribution for flow arrangement B. $\xi = 0.8$ and $Hu = 0.3$

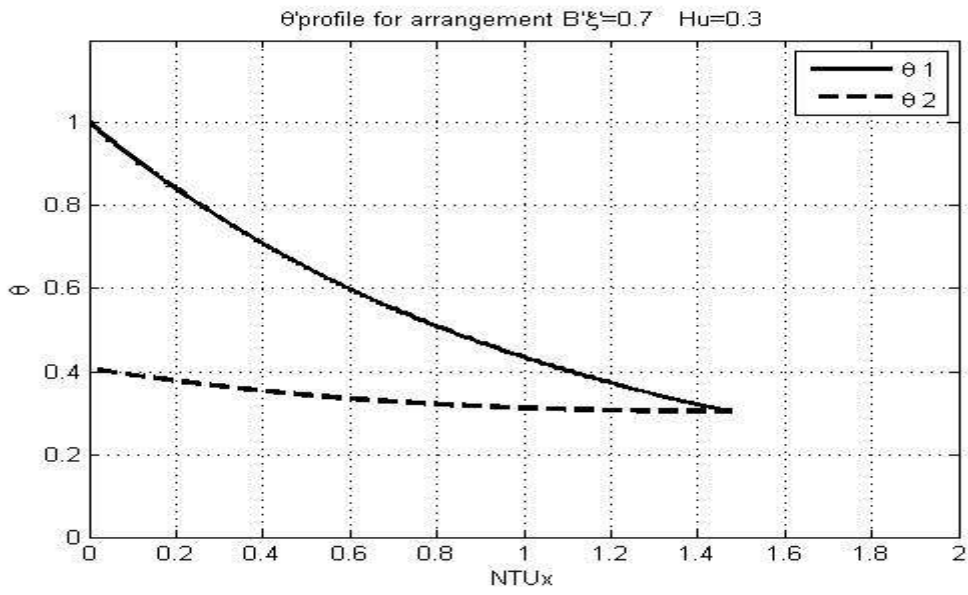


Figure 2.9: Temperatures distribution for flow arrangement B. $\xi = 0.7$ and $Hu = 0.3$

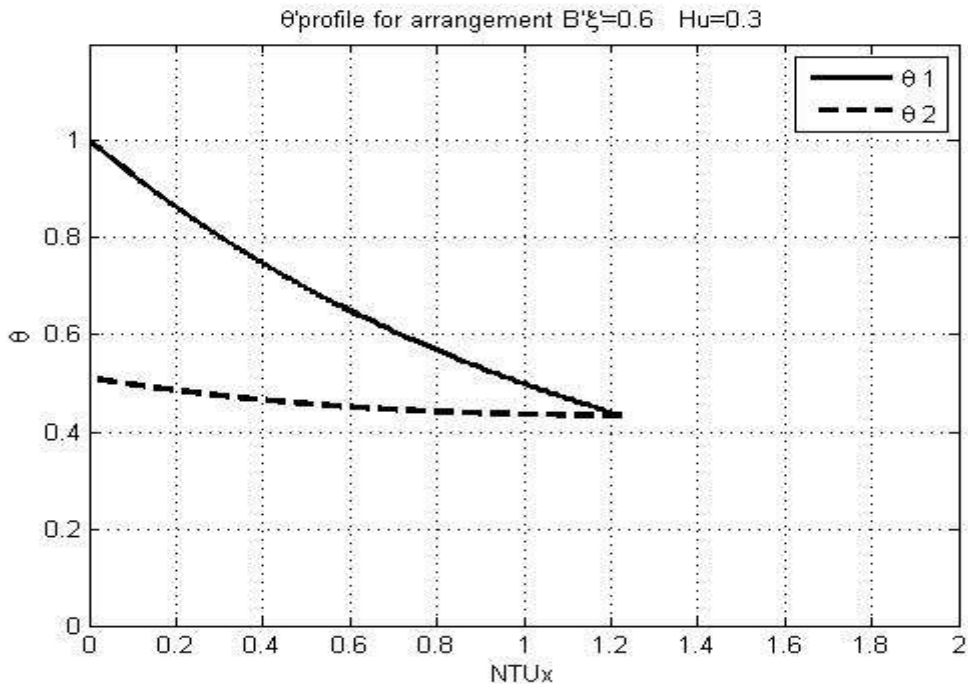


Figure 2.10: Temperatures distribution for flow arrangement B. $\xi = 0.6$ and $Hu = 0.3$

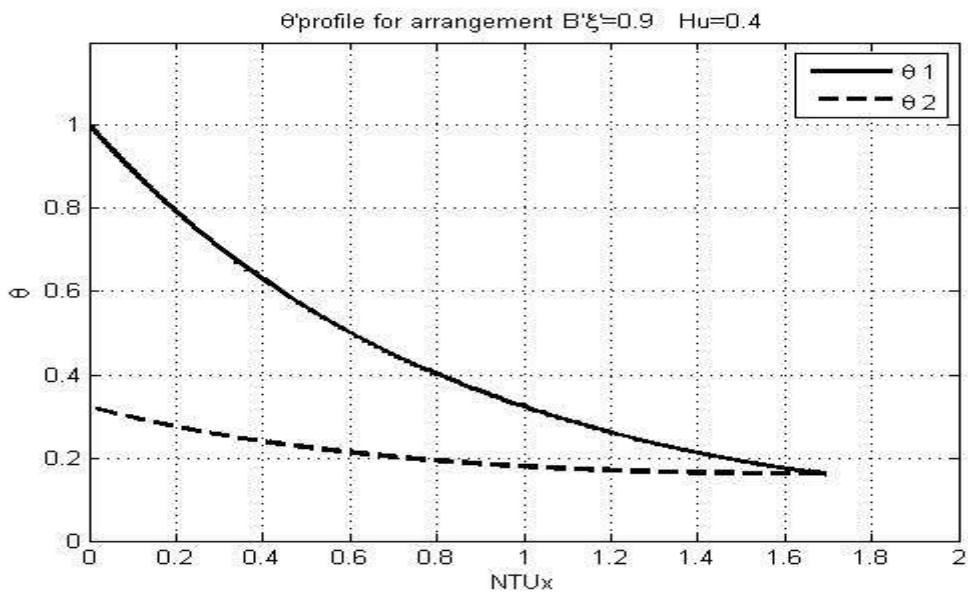


Figure 2.11: Temperatures distribution for flow arrangement B. $\xi = 0.9$ and $Hu = 0.4$

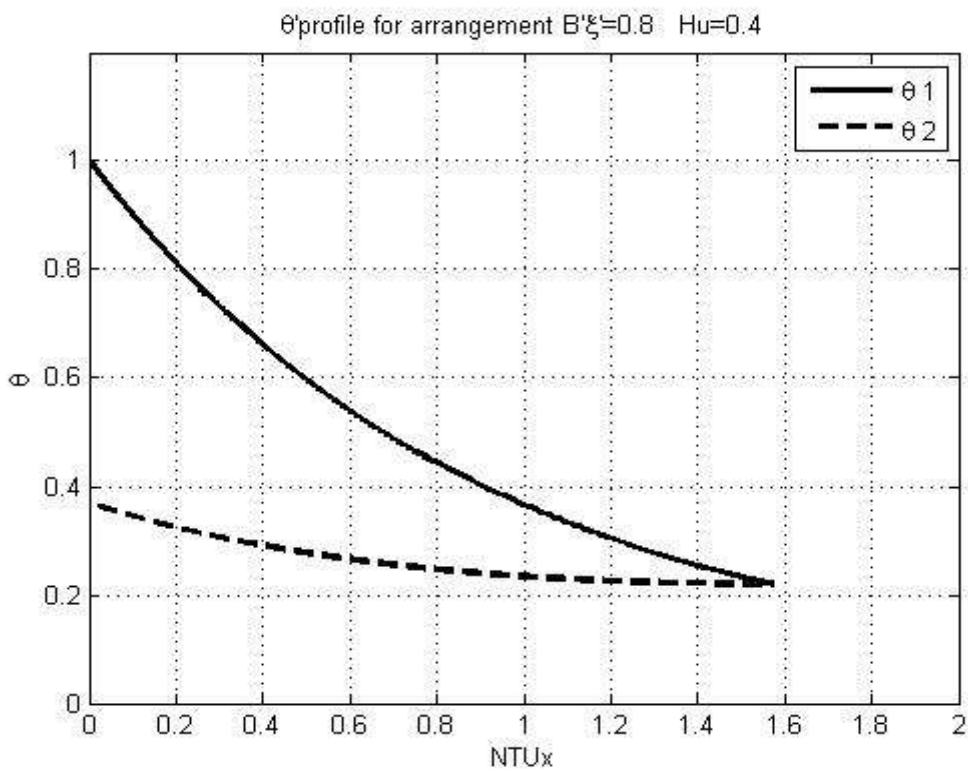


Figure 2.12: Temperatures distribution for flow arrangement B. $\xi = 0.8$ and $Hu = 0.4$

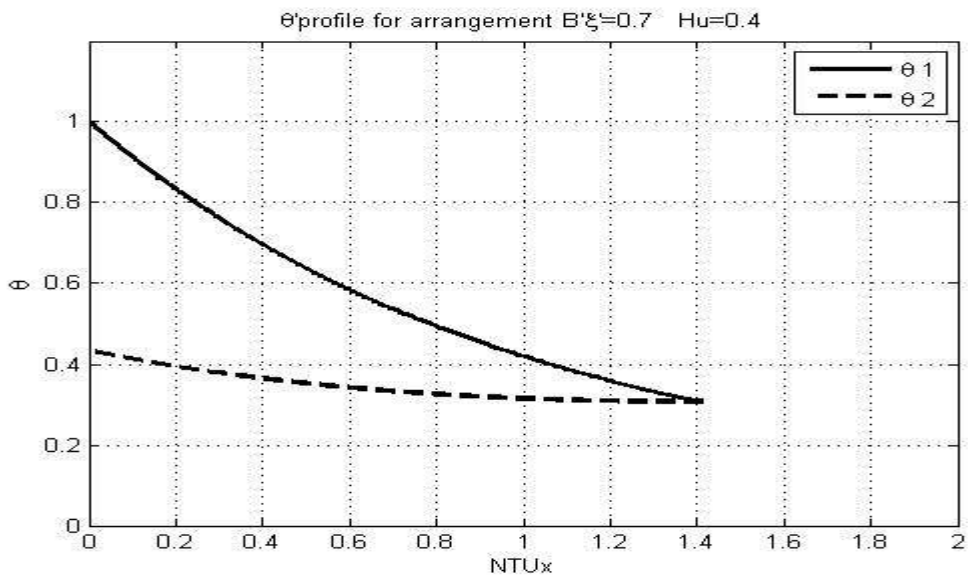


Figure 2.13: Temperatures distribution for flow arrangement B. $\xi = 0.7$ and $Hu = 0.4$

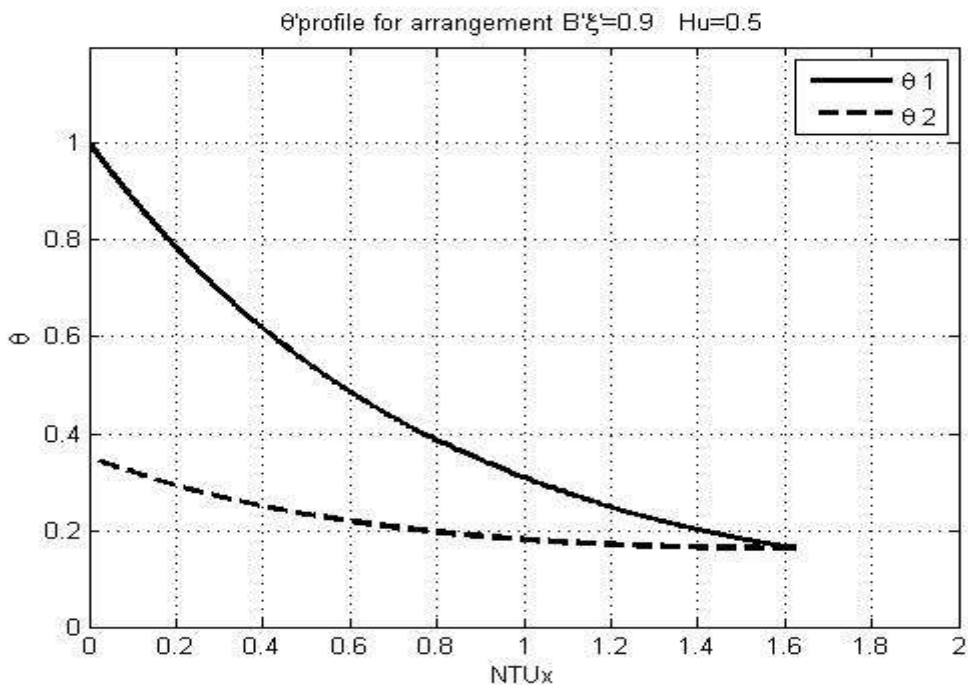


Figure 2.14: Temperatures distribution for flow arrangement B. $\xi = 0.9$ and $Hu = 0.5$

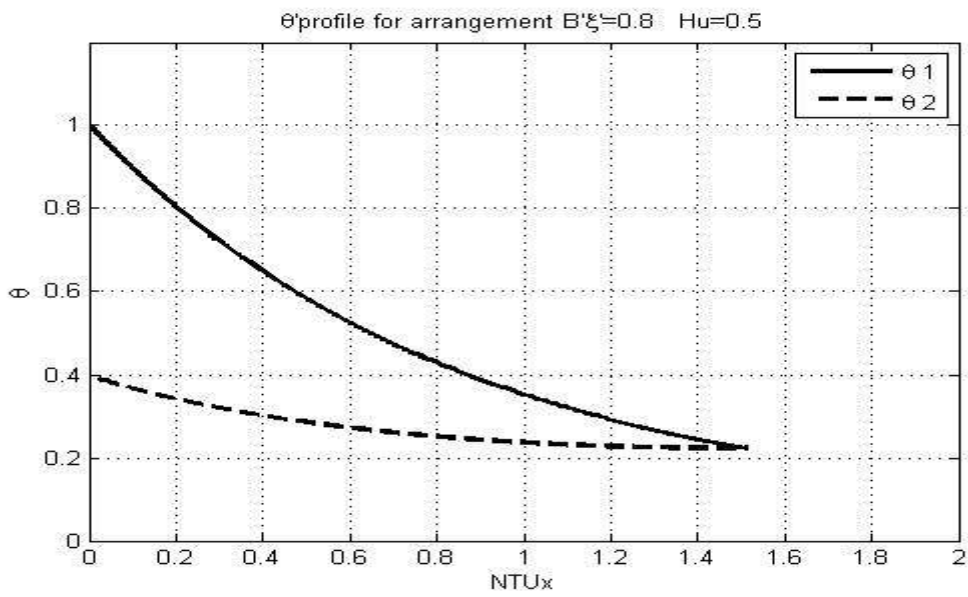


Figure 2.15: Temperatures distribution for flow arrangement B. $\xi = 0.8$ and $Hu = 0.5$

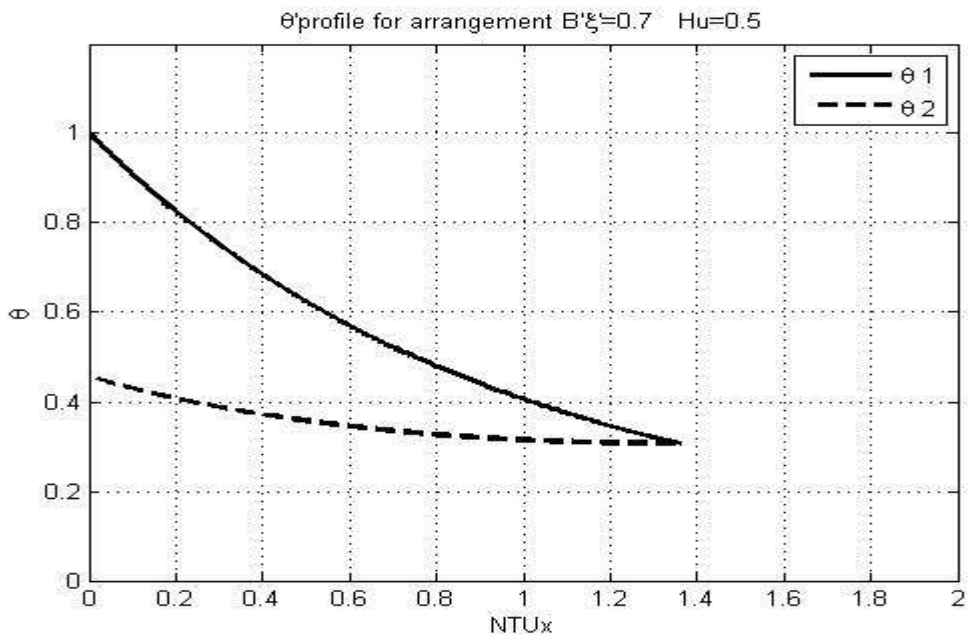


Figure 2.16: Temperatures distribution for flow arrangement B. $\xi = 0.7$ and $Hu = 0.5$

